



Met Office

Diurnal Variability in Sea Surface Temperature: Observation and model assessment

Forecasting Research Technical Report 556

June 2011

Peter Sykes, James While, Alistair Sellar, Matt Martin

Abstract

Satellite and buoy observation platforms have been assessed for their ability to resolve the diurnal cycle of sea surface temperature (SST). Moored buoy hourly time series are examined and satellite data assessed against drifter buoys. The moored buoys show that 4 evenly spaced observations per day are required to resolve the SST diurnal cycle in order to satisfy the Nyquist sampling requirements. Satellites are only able to achieve this level of observation frequency if they are geostationary and are sampling areas unaffected by cloud cover. Nevertheless, statistical assessment of the satellite data showed that a diurnal signal is detectable.

The Met Office's ORCA025 (global) configuration of NEMO (Nucleus for European Modelling of the Ocean) -FOAM (Forecasting Ocean Assimilation Model) has been assessed for its ability to simulate a diurnal cycle of SST. Hourly SST output from the model is compared to in-situ buoy (PIRATA) and geostationary satellite (SEVIRI) SST measurements. An algorithm is used to identify daily diurnal SST minima, maxima and ranges for the observations and model data over a 1 month period in July 2008. The timings of the diurnal minima and maxima within the buoy and model data are also compared.

The assessment showed that FOAM does produce a diurnal cycle with skill across all forecast days, albeit with an increase in bias and decrease in correlation with increasing forecast time. The model maxima and minima timings tend to be of the order of 1 hour late compared to the buoy data. Diurnal ranges produced by FOAM tend to be underestimated relative to the satellite values, this potentially being due to no skin correction in the model and 6 hourly rather 3 hourly flux forcing.

Contents

| | |
|--|-----------|
| Abstract | 1 |
| Contents | 2 |
| Executive Summary | 3 |
| Introduction | 4 |
| Observations | 6 |
| Observations Used | 6 |
| NOAA-AVHRR | 8 |
| METOP-AVHRR | 8 |
| SEVIRI | 9 |
| In-situ Data..... | 9 |
| Sampling requirements..... | 10 |
| Matchup Analysis | 15 |
| Model Assessment | 20 |
| Model Experimental Setup | 20 |
| Model and Buoy Comparisons | 21 |
| Observations Used | 21 |
| Procedure | 22 |
| Hourly Time Series | 23 |
| Diurnal Maxima, Minima and Ranges | 24 |
| Maxima and Minima Timing..... | 26 |
| New Zealand Buoy Assessment..... | 28 |
| Model and Satellite Comparisons..... | 31 |
| Procedure | 31 |
| Statistics Maps..... | 32 |
| Domain-Average Statistics..... | 36 |
| Conclusions | 37 |
| Future Work and Recommendations | 39 |
| References | 40 |

Executive Summary

As part of our commitment to the DEfence Research Technology Program (DERTP) we have studied the capability of both observations and the Met Office's Forecasting Ocean Assimilating Model (FOAM) to resolve the diurnal cycle of Sea Surface Temperature (SST).

By examining time-series obtained from moored buoys we have found that 4 evenly spaced observations per day are required to resolve the SST diurnal cycle. Given the available satellite data, this level of observation frequency was found to occur only in regions monitored by geostationary satellites, and then only in small, cloud free, areas. Furthermore, when matched to drifter measurements, satellite SST observations show errors similar in magnitude to diurnal variability. Nonetheless, when analysed statistically a diurnal signal was detectible in satellite data.

The FOAM model, which has global coverage, has been found to generate a diurnal cycle in SST. Results from comparing 5-day FOAM forecasts to moored buoy and geostationary satellite observations have been mixed, with the model performing better in some areas than others. On average, the model forecasts, regardless of lead time, do well at predicting the time of maximum and minimum SST; however, the timings tend to be late by approximately 30-60 minutes. The forecasts do less well at calculating the diurnal range, which is underestimated, sometimes substantially. It has been found that some of this underestimation comes from updates to the meteorological forcing being too infrequent. A further cause of error is the difference between the true 'skin' SST and FOAM's SST, which is an average of the temperature in the top 1m of the ocean. Nonetheless, FOAM does have some skill at predicting the diurnal cycle and, with its limitations kept in mind, is capable of producing a usable diurnal SST forecast.

The study reported here has highlighted the need for further developments in the representation of diurnal SST using both observations and FOAM. In particular, a global diurnal SST analysis product could be developed, whereby observations are combined with a diurnal model that exists on top of, and is consistent with, the OSTIA SST analysis. Such a system would overcome many of the sampling problems inherent in SST data. Additionally, development of a correction to convert model SST to skin SST in FOAM should greatly improve the diurnal forecasts it provides. Furthermore, A recent

operational upgrade (too late for inclusion in this report) to using 3 hourly meteorological forcing, instead of 6 hourly, should already have improved FOAM's diurnal SST.

Introduction

As part of its commitment to the DEfence Research Technology Program (DERTP) the Met Office is conducting a study into the diurnal cycle of Sea Surface Temperature (SST). The ultimate aims of this work are:

1. To improve SST inputs to NWP modelling of radar ducting. Results of previous work in this area have been reported in Wang (2010).
2. To improve the estimates of SST used by the NEON target model. This target model determines a ships visibility in the infra-red by comparing hull temperature to SST.
3. To improve SST inputs to models of evaporative ducting.

The work discussed in this document is aimed at addressing some of the issues associated with the points above. Specifically, this report aims to clarify our current ability to determine the diurnal cycle of SST. This is done by both examining the ability of satellite observations to determine the diurnal cycle, and by validating the diurnal cycle of the Met Office's Forecasting Ocean Assimilating Model (FOAM). Results from this report will be used to guide future developments in both of these areas.

Before moving on to a discussion of diurnal cycles, it is important to define what we mean by SST. In this report we try to follow the standardised system in use by the Group for High Resolution SST (GHRSSST; see <http://www.ghrsst.org/>), and summarised in Figure 1. In this standard there is an 'interface' SST overlaying first the 'skin' SST (measured by infra-red sensors), and then the 'sub-skin' SST (measured by microwave instruments). At depths of order 1m is the region sampled by in-situ instruments, where the depth of observation should always be stated; finally there is the 'foundation' SST which is the region below any diurnal cycle in temperature. The actual temperature profile through these regions can vary significantly depending upon ambient conditions, with two possible profiles shown in Figure 1.

The diurnal cycle of SST is caused by the direct daytime solar heating and night time cooling of the top few meters of the ocean. This cycle can be considered to be on top of

long period seasonal changes and variability due to advective and mixing processes. In the absence of wind, cloud, and precipitation, the SST diurnal cycle would follow a predictable oscillatory pattern. However, variations in solar heating due to cloud and the tendency of wind to mix heat to depth, make the diurnal system much more complex (see Webster, 1996 for a detailed discussion of these processes). This complexity leads to large variations in the magnitude of the SST diurnal cycle, as is shown globally in Stuart-Menteth et al (2003) and Gentemann et al (2003), and more regionally in Clayson & Weitlich (2005) and Merchant et al (2008). Although they are beyond the scope of this report, it is of note that there have been numerous attempts to create 1-dimensional models of diurnal SST, including: Price & Weller (1986), Webster (1996), Fairall et al (1996), and Schiller & Godfrey (2005). In the future diurnal models such as these may present a way for us to develop our systems for analysing the diurnal cycle. Of particular interest is the possibility of creating an analysis of the diurnal cycle in the context of the Met Office's OSTIA analysis (Donlon et al, in press). In such a system OSTIA would be used to provide an estimate of foundation SST to a diurnal model.

This report has a two part structure, with the first part focusing on an analysis of observations and the second part concerned with the modelled diurnal cycle in FOAM. In the first part of the report we give a brief overview of each available observation type, before presenting the results of a study into the ability of satellite observations to resolve diurnal variability. Also in the first part of the report we discuss the results of a matchup analysis between satellite data and co-located drifter data, conducted in order to assess the errors in satellite diurnal SST.

The second part of this report begins with a description of the FOAM system and the experiments conducted to test its diurnal SST output. The observations used to validate these experiments are summarised, before results of time-series comparisons between observations and model are given. Furthermore, a procedure for comparing the model to the data, describing the SST minimum, SST maximum, and diurnal range are presented. The final part of the report details our conclusions and outlines plans for possible future developments.

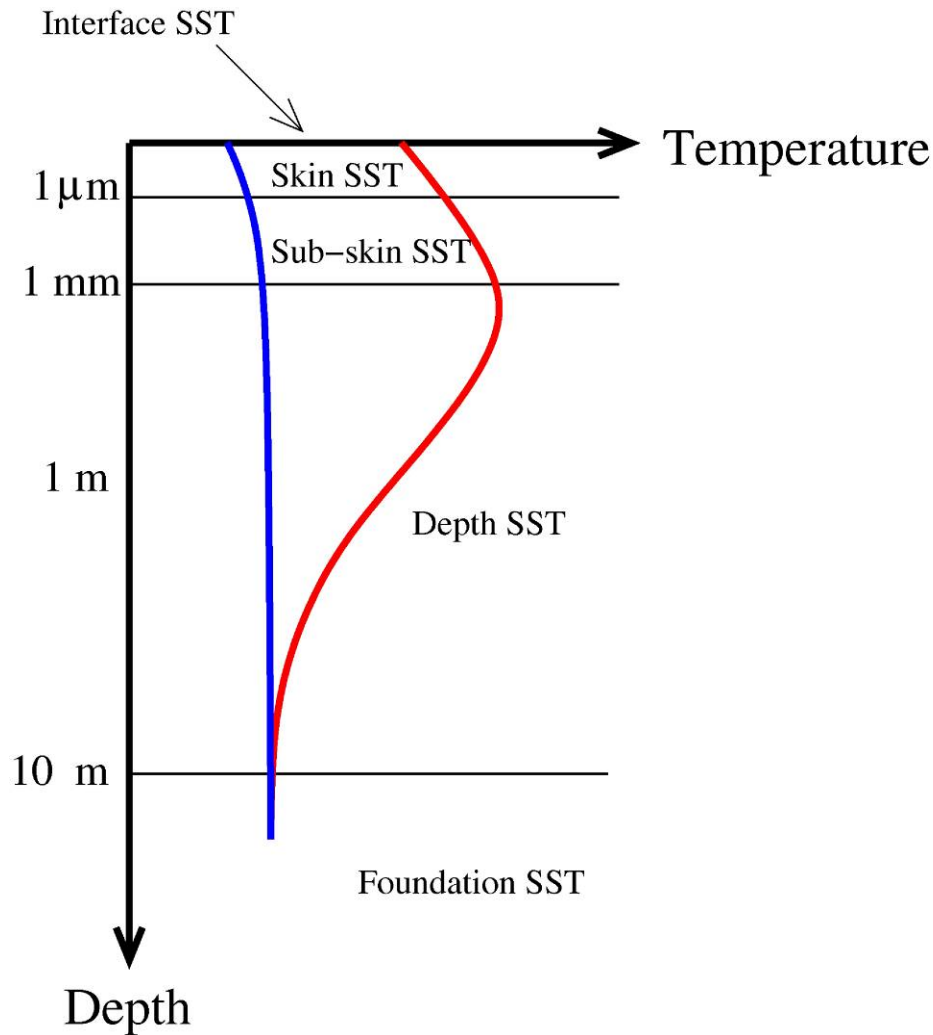


Figure 1: Definitions of SST as defined by the GHRSSST. Note that Depth SST simply refers to the need for a precise depth to be given for measurements in this zone. The blue and red lines show, respectively, example temperature profiles for night-time (or high wind) and low wind, high insulation conditions.

Observations

Observations Used

In order to study diurnal SST it is first necessary to compile and obtain suitable data. Early in the project it was decided to concentrate on in-situ data and satellite infra-red measurements of temperature. Microwave instruments were discounted as they are only sensitive to the sub-skin SST, not the skin temperature, and it was believed that their large measurement footprint and lower accuracy rendered them unsuitable for diurnal SST work. Also discounted were the GOES-East and GOES-West geostationary satellites; this was due to their poor SST response during daylight hours (see OSI-SAF, 2006). Given these constraints, available observational data included

data from 4 satellite sources – AATSR, AVHRR-NOAA, SEVIRI, and AVHRR-METOP – and in-situ data from moored buoys, voluntary observing ships, and drifters. Data from the geostationary satellite MT-SAT (which is centred above the west Pacific) was also considered, but a data stream from this satellite was not available in time to be included in this study. Nonetheless, MT-SAT is likely to be an important data source in the future. A further satellite observation stream, from the recently launched COMS satellite (see http://events.eoportal.org/get_announce.php?an_id=10928), is also likely to be a significant future data source.

Data from all available sources were extracted for the months of July 2008 and February 2009. However, July 2008 was chosen to be our principal study period and unless otherwise stated all results presented here come from this month. Once extracted the data were quality controlled via a comparison to the Levitus climatology (Levitus, 2006) using the Bayesian methodology of Lorenc & Hammon (1988) and Ingleby & Huddleston (2007). This is the same as the operational quality control system used at the Met Office for OSTIA and FOAM. However, the quality control was weakened to allow for the large diurnal differences (up to 4.5 K, see Stuart-Menteth et al, 2005) that can exist between satellite skin measurements and the SST measured by buoys at depth; a signal we did not want removed from our results. The quality control assumes that SST measurements are at depth and we therefore calculated that the background error variance needed to be increased by $2.7K^2$ to prevent satellite observations being quality controlled out of the data set. As an additional processing step we also converted the reference time of all observations to mean local time (i.e., universal coordinated time + [longitude / 360°]).

A more detailed examination of the individual data types discussed in this report is given below. It should be noted that all satellite data were obtained by this project through the GHRSSST.

The European Space Agency (ESA) -Advanced Along Track Scanning Radiometer (AATSR) is a 3 channel (11 μ m, 12 μ m and 3.7 μ m) infrared instrument mounted aboard the Envisat satellite. Envisat circles the Earth in a sun synchronous polar orbit with an equator crossing time of 10:00am; as a consequence AATSR only samples a relatively small portion of each day and night. Unlike the other satellite instruments described here, AATSR SSTs are not directly calibrated to drifter data. Instead the instrument is calibrated to internal black bodies, and a dual view system is used to reduce the impact

of atmospheric absorption and emission on the calculated SSTs. It is this factor that results in the AATSR instrument having a lower bias than its contemporaries. Additionally, because of its internal calibration system, AATSR is set-up to return the ocean skin temperature, not the SST at depth. A consequence of the dual view system is that AATSR has a much narrower swath (about 500km) than other infra-red instruments. Further information on AATSR is available at <http://envisat.esa.int/handbooks/aatsr/CNTR1.htm#eph.aatsr.ug>.

NOAA-AVHRR

The Advanced Very High Resolution Radiometer 3 (AVHRR-3) is an infra-red radiometer mounted onboard a sequence of NOAA satellites. As with AATSR, these satellites all follow a polar orbit. Six infra-red channels are used to obtain the SST by fitting an empirically derived function to the observed radiances. The coefficients for this function were derived by comparing NOAA-AVHRR brightness temperatures to SST data from drifters. NOAA-AVHRR radiometers have a much wider swath (~2,500 km) than the AATSR instrument. For a detailed description of the NOAA AVHRR instrument see <http://www2.ncdc.noaa.gov/docs/klm/html/c3/sec3-1.htm>

The NOAA-AVHRR data used in this report is the Global Area Coverage (GAC) data set, which provides data at 4km resolution. Although there are normally two NOAA-AVHRR instruments operational at any one time, only the data from one instrument (NOAA – 18) was used in the generation of the results presented in this report.

METOP-AVHRR

The METeorological OPERational (METOP) satellite program is a European sun-synchronous polar orbiting satellite that contains an AVHRR instrument. As with NOAA-AVHRR, an empirically derived function is used to convert the observed radiances to SST. However, the processing algorithm is different from that used by NOAA-AVHRR and the data are provided at a higher (1km) resolution. METOP-AVHRR data are also generally considered to be more accurate than NOAA-AVHRR. Further information on the METOP-AVHRR product is given in OSI-SAF, 2010.

SEVIRI

The Spinning Enhanced Visible and Infrared Imager (SEVIRI) is an infra-red SST sensor mounted onboard the Metosat Second Generation (MSG) geostationary satellite. The satellite is positioned above the equatorial Atlantic and provides continuous SST data for most of the Atlantic between 60S and 60N. Details of the SEVIRI instrument can be found at <http://www.esa.int/msg/pag4.html>.

For this project we used a preliminary version of an hourly SEVIRI SST product, which is described in Le Borgne et al (2011). As a geostationary instrument SEVIRI can, in the absence of cloud, provide high temporal resolution coverage of SST in its observation region. It is this ability to provide continuous coverage which makes SEVIRI extremely valuable for diurnal studies. However, because of its distance from the Earth, SEVIRI is both less accurate and of a lower (6km) resolution than the other satellites. Furthermore, as it is geostationary, SEVIRI only ever records data from the same region of the Earth and does not provide global coverage.

In-situ Data

A wide range of in-situ data sets was available to this project. The bulk of this data was available from the Met Office's observation database (MetDB) and included data from drifters, moored buoys, and voluntary observing ships. Observations from in-situ platforms can be considered to be measurements of the SST at various depths, with a typical measurement depth of 1m.

Two additional in-situ data sources were extracted to complement the data available from the Met Office database. The first of these were data from the TAO, PIRATA, and RAMA equatorial moored buoys (see <http://www.pmel.noaa.gov/tao/>). These buoys provided hourly data at a number of locations near the equator in the Pacific, Atlantic, and Indian oceans respectively. While available on the Met Office's database, we obtained the TAO, PIRATA, and RAMA data directly from the above website, where it was available at a higher temporal resolution. The other data source was two weeks of high temporal resolution data (15 minute sampling interval) available from a buoy located off the coast of New Zealand at 37.8S, 179.8E. The New Zealand data was available for the period 22nd February – 7th March 2009, and so is not included in the

bulk of the results below; however, it was useful as a high resolution time-series to be used in our investigations.

Sampling requirements

In order to resolve the diurnal cycle with satellite information, the data must be accurate enough to measure the diurnal signal and frequent enough to capture the diurnal variability. Figure 2 shows a time series example that illustrates these points. In this figure we show a pair of time series from two Atlantic PIRATA buoys compared to time series of area averaged (0.25° , 1° and 1.5° averaging) SEVIRI data. The plots in this figure are typical of what is observed at many of the moored buoys. The bottom plot shows, as is common, what happens when there is insufficient data to sample the diurnal cycle and there are large data gaps in the signal. For most of this plot it is effectively impossible to reconstruct a diurnal cycle from the satellite data. The top plot, in contrast, shows the results when good temporal coverage is available from the satellite. A diurnal cycle is clearly visible in the satellite data throughout the period, and while there are significant errors for the first part of the month, the 0.25° satellite data shows good agreement with the buoy for the last 15 days of the plot. However, it is worth noting that when averaging over a large spatial area the satellite data significantly overestimates the range of the diurnal cycle. This is presumably due to the diurnal cycle having a much larger range elsewhere within the averaging area than is represented by the buoy.

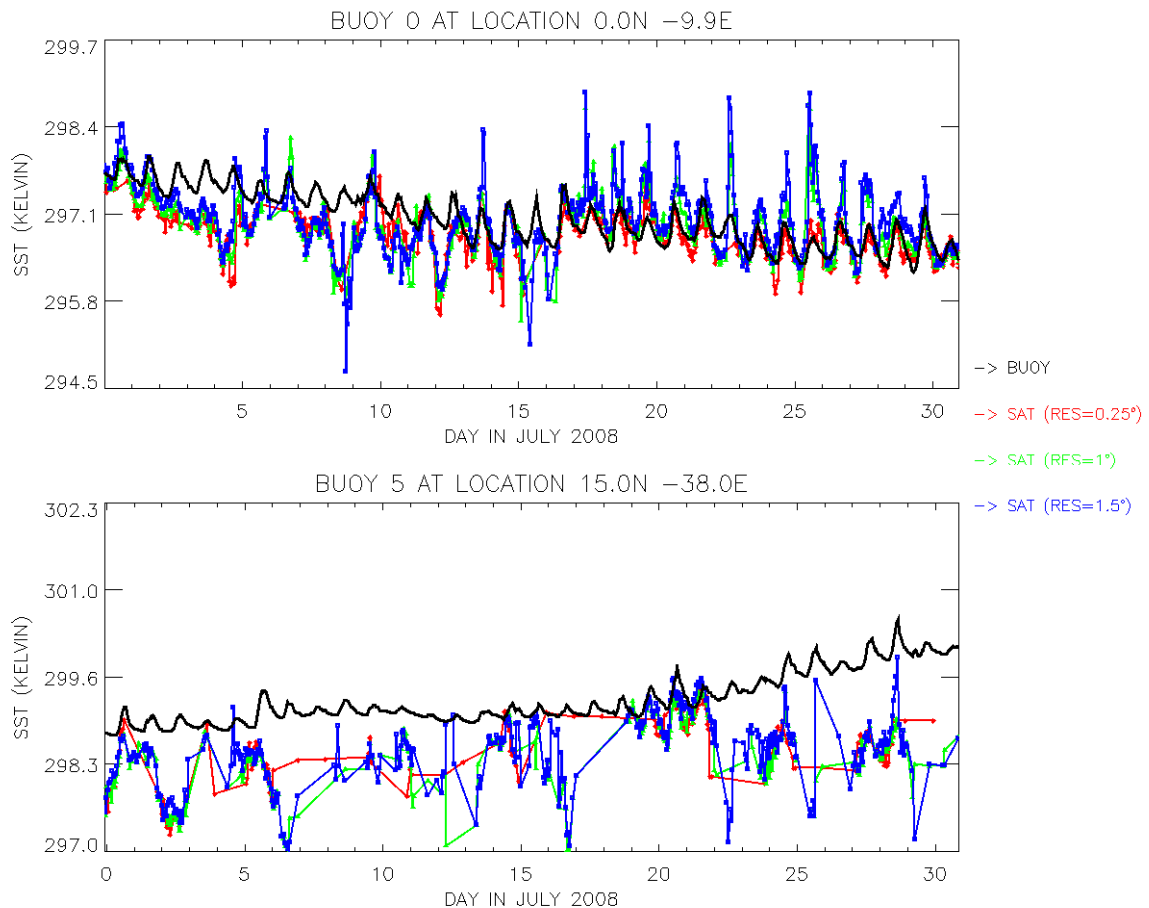


Figure 2: Time-series of moored buoy data (black line) against a distance weighted average of nearby satellite data. Three averaging radii were used: 0.25° (red line), 1° (green line), and 1.5° (blue line). The top plot shows a buoy where good satellite coverage was available, while the bottom plot shows the situation when satellite coverage was poor.

It is a fundamental property of time series (see Percival & Walden, 1993 for a discussion on the theory of time series) that to resolve a signal you must sample the signal faster than twice the highest frequency present. As a consequence, if a diurnal signal is purely sinusoidal, then it can be resolved by evenly spaced samples separated by just less than 12 hours. However, diurnal signals are more complex than pure sinusoids and in order to discover the maximum frequencies present we calculated periodogram (see Percival & Walden, 1993) estimates of the Power Spectral Densities (PSDs) of a number of time series from moored buoys. In all cases a linear trend was removed from the signal before calculating the PSD. Results of this analysis for the New Zealand buoy and a buoy from the Atlantic PIRATA array are shown in Figures 3 and 4 respectively. For the New Zealand buoy a strong sharp diurnal peak is seen at 0.042 cycles/hr (corresponding to a wavelength of 1 day), with a small amount of power bleeding over to ~ 0.1 cycles/hour. The PIRATA buoy also shows a strong diurnal peak, but also displays

detectable peaks at 2 and 3 cycles/day. The 3 cycles/day peak is too small to significantly alter the diurnal signal; however, the 2 cycles/day peak, which has been observed to be larger in other buoys, is almost at the 0.01K^2 level (corresponding to a 0.1K amplitude waveform) that might be detectable via satellite. As a consequence we believe that this 'semi-diurnal' peak must be captured to resolve the diurnal cycle. By implication at least 4 samples, evenly spaced, of SST are required each day. These results are consistent with Gentemann et al (2003) which used a Fourier series to model the diurnal cycle and found that only the first two harmonics are significant; however the Fourier series did contain power out to the 5th harmonic, which we have not observed.

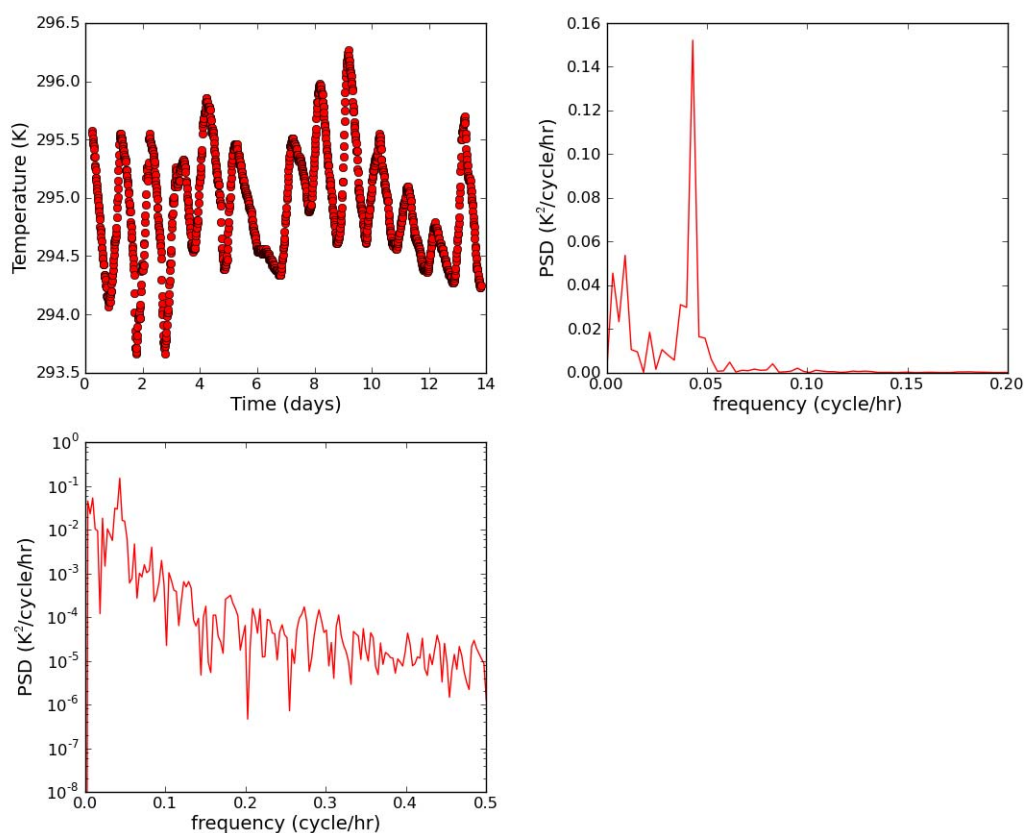


Figure 3: Power Spectral Density (PSD) of the data from the New Zealand Buoy (located at 37.8S, 179.8E). The top left plot shows the time-series of the data, while the top right plot shows the PSD of the detrended time-series. The bottom plot shows the PSD on a log scale. All data were processed as described in the text.

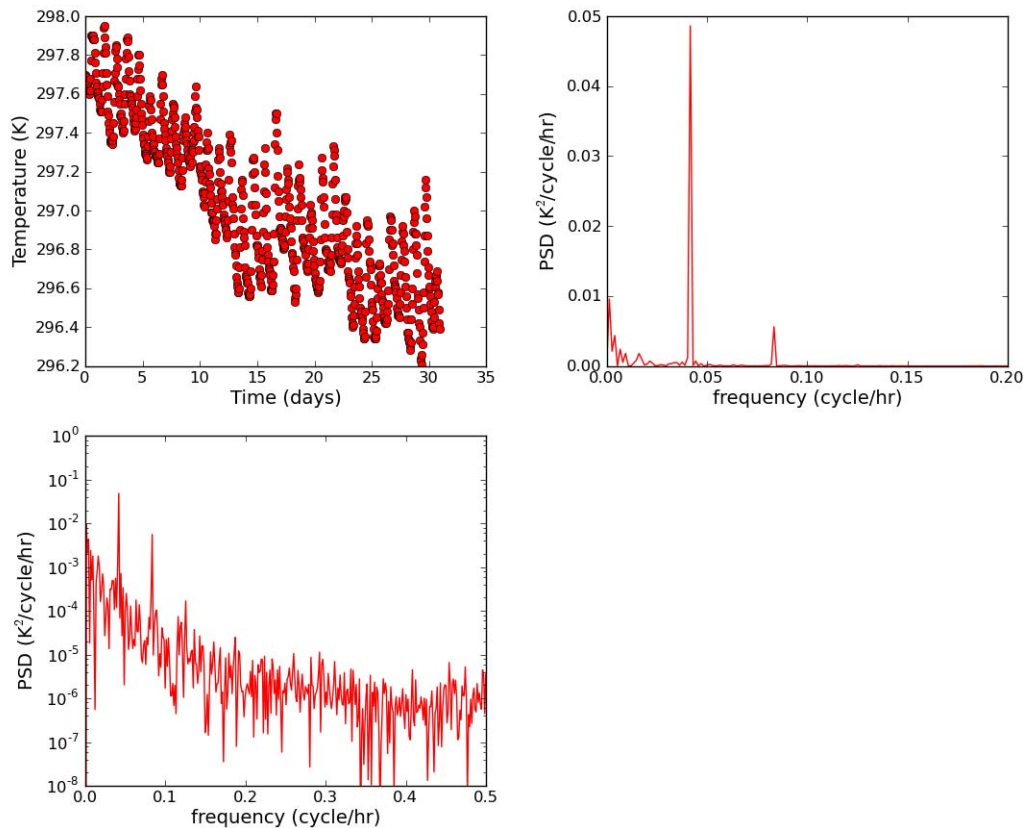


Figure 4: Power Spectral Density (PSD) of the data from a buoy located at 0N, 10W (part of the PIRATA array). The top left plot shows the time-series of the data, while the top right plot shows the PSD of the detrended time-series. The bottom plot shows the PSD on a log scale. All data were processed as described in the text.

In order to assess how often adequate, 4 times daily, sampling occurs we divided the day into four 6 hour periods (00:00 – 06:00, 06:00 – 12:00, 12:00 – 18:00, and 18:00 – 24:00) and checked to see if they contained an observation. Only if all 4 periods contained an observation did we consider the diurnal cycle to be adequately sampled. Figure 5 shows the results of performing this analysis on the available satellite data in a 0.25°x0.25° grid. The top plot of this figure shows the mean number of time periods filled per day when averaged over July 2008, while the bottom plot shows the number of days on which the diurnal cycle could be considered resolved (i.e., all 4 time periods contained at least 1 observation). It is immediately apparent that over most of the globe adequate sampling is rare. Only in the region covered by SEVIRI (i.e., the Atlantic), and then not everywhere, is the diurnal cycle sufficiently sampled on half the possible days. Elsewhere, the diurnal cycle is resolved, at best, on only a few days during the month. This indicates the huge potential problems in determining the diurnal cycle on any

particular day directly from satellite data. In regions without continuous geostationary coverage the problem is probably intractable and still difficult even with geostationary data. One interesting point from Figure 4 is that much of the ocean has, on average, at least one observation per day; this implies that, while the diurnal cycle is not resolved, longer period changes are well constrained by satellite measurements.

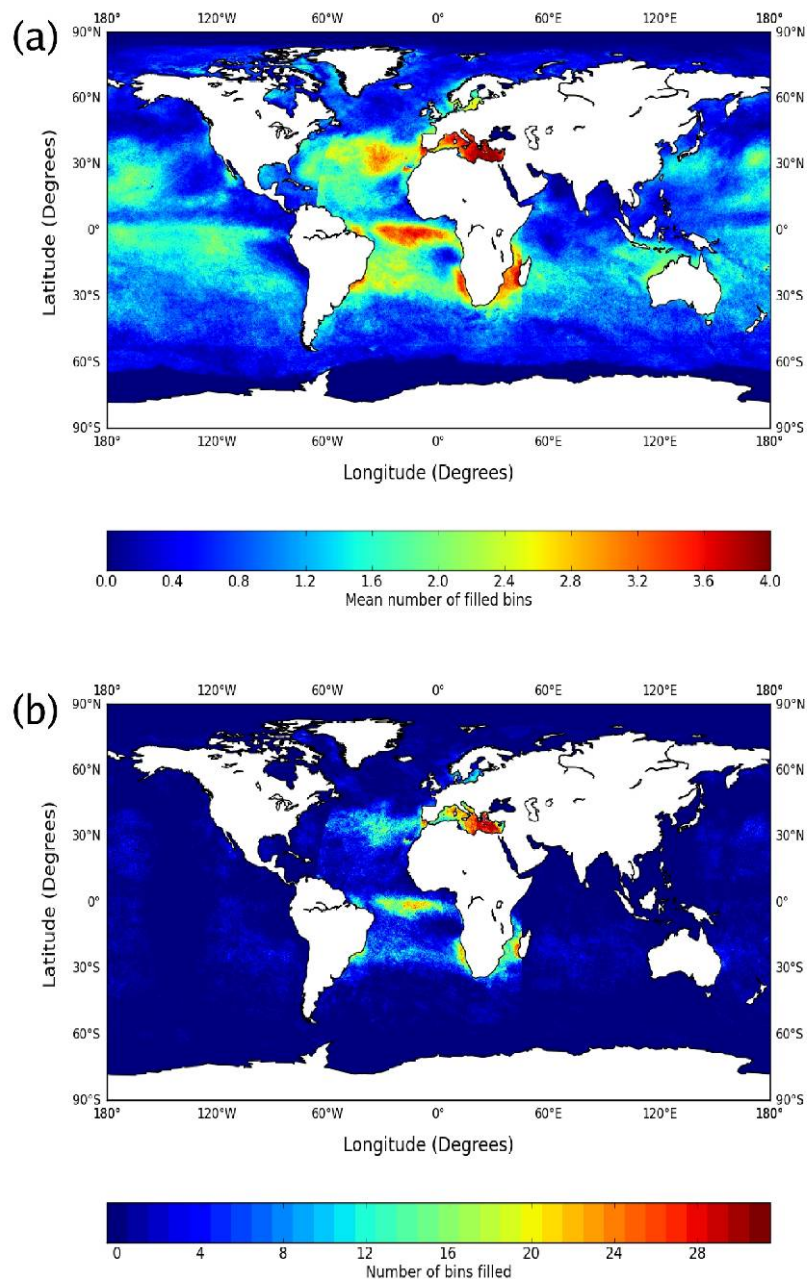


Figure 5: Global sampling coverage by all satellites for July 2008. (a) Mean number of daily quarter periods observed (see text for details); (b) Number of days when all quarter periods were observed. Results shown are for a 0.25°x0.25° grid.

Matchup Analysis

As shown above, satellite data are of generally too low temporal resolution to resolve the diurnal cycle. Nonetheless, statistical information, such as the mean diurnal cycle and error analyses, can still be extracted from satellite measurements. Such analyses still require satellite data to be of sufficient quality, in terms of signal to noise characteristics, to discern diurnal changes. One way to explore the noise properties of satellite data is to generate a matchup database between satellite and in-situ observations and analyse the difference between the two data sources. We have generated such a matchup database between our satellite data and drifters and it is the analysis of these matchups that is the subject of this section.

In calculating the matchups we only considered the nearest satellite datum to a drifter observation, where the measurements had to be within 10km and 90 minutes of each other. A plot of the matchups for July 2008 is given in Figure 6, with statistics for the global matchups given in Table 1. Also given in the table are the statistics for matchups from February 2009.

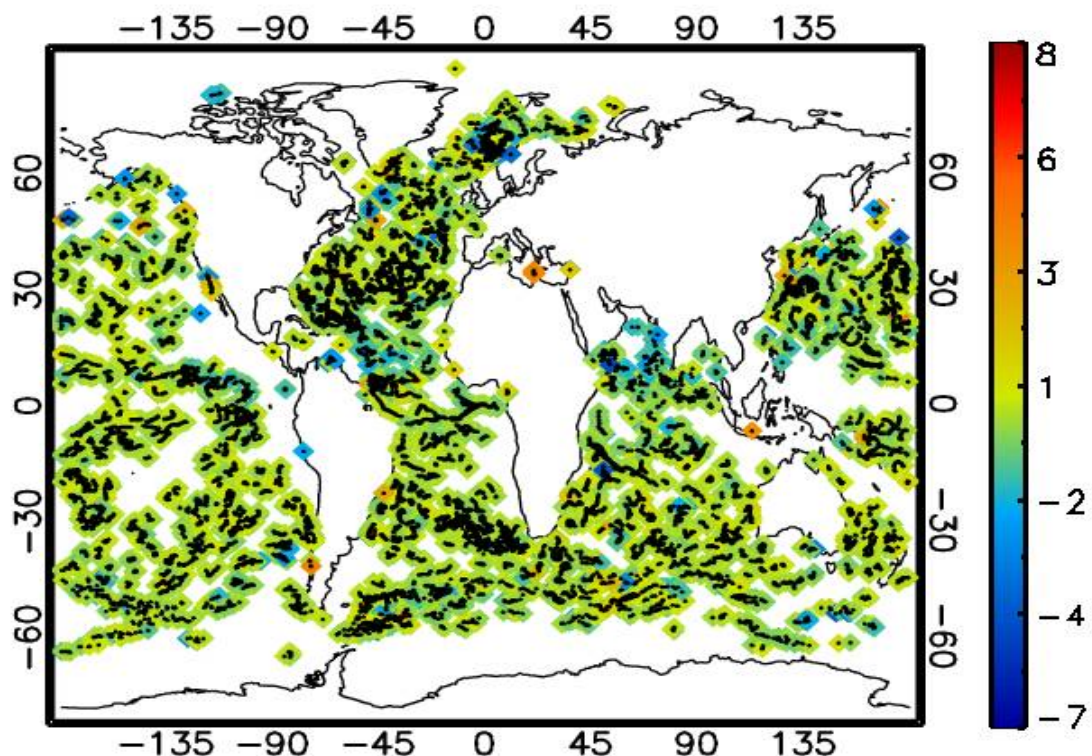


Figure 6: Location of matchups between satellites and drifter data for July 2008. All matchups were within 10km and 90 minutes of each other. Black dots mark the position of the matchups, while the coloured diamonds show the matchup temperature difference in Kelvin.

| Satellite instrument | Mean difference (K) | | Standard deviation (K) | |
|----------------------|---------------------|--------|------------------------|--------|
| | July 08 | Feb 09 | July 08 | Feb 09 |
| AATSR | 0.02 | 0.07 | 0.62 | 0.53 |
| NOAA-AVHRR | 0.07 | 0.06 | 0.47 | 0.43 |
| SEVIRI | -0.04 | 0.12 | 0.68 | 0.42 |
| METOP-AVHRR | 0.09 | 0.11 | 0.63 | 0.60 |

Table 1: Global matchup statistics between satellite and drifter observations.

From the statistics in Table 1, it is clear that the satellite data does a reasonable job at capturing the SST, with both the mean differences and standard deviations always less than 1K. It should be noted, however, that with the exception of AATSR the bias is artificially low; this is because NOAA-AVHRR, METOP-AVHRR, and SEVIRI are all directly calibrated against drifters (if, as well as drifters, the statistics are calculated against all in-situ data then the biases are significantly increased; for July 2008: AATSR: 0.04K, NOAA-AVHRR: 0.12K, SEVIRI: 0.06K, METOP-AVHRR: 0.19K). Also of note is the large change in the mean error of AATSR between July 2008 and February 2009. Further investigation (results not shown) has found that the behaviour of this data set differs significantly between the two months. At the time of writing it is not clear what has caused this change in behaviour.

A close inspection of the standard deviations shown in Table 1, reveals that they are relatively large compared to the diurnal signal in many parts of the ocean. Typical values are about 0.5K, while, for instance, the peak to trough diurnal signal amplitude at the New Zealand buoy is 0.8K. While an intelligent use of data averaging will reduce the noise in satellite data, the comparatively large errors in single observations should be borne in mind when trying to analyse the diurnal signal in limited data.

To determine if satellite data can resolve a diurnal cycle comparable to that detected by the drifters, we binned all available matchups of SEVIRI data into 20°x20°x6 hour bins. Within these bins we calculated the mean SST for both the satellite and the drifters, along with their mean differences. The results of this calculation are shown in Figure 7 and are quite noisy, especially where the number of matchups is small. The likely reasons for the noise are spatial inhomogeneities in SST across the grid cell. However, in some regions, most prominently between the equator and 40N, a diurnal cycle can be

seen in the satellite data. This is evidenced by cold mornings followed by a temperature increase in the following two periods of the day, before a cooling during the night. This pattern is closely followed by the drifter data (Figure 7b) indicating that the satellite is picking out the same diurnal signal as the drifters. Interestingly, the difference between the satellite data and the drifters does not follow this pattern. As satellites only measure the skin temperature, and drifters only measure the temperature at depth, an increase in error during periods of intense solar heating might be expected, but is not observed. As a result we speculate that the diurnal cycle of error for SEVIRI is too small relative to other error sources to be detected.

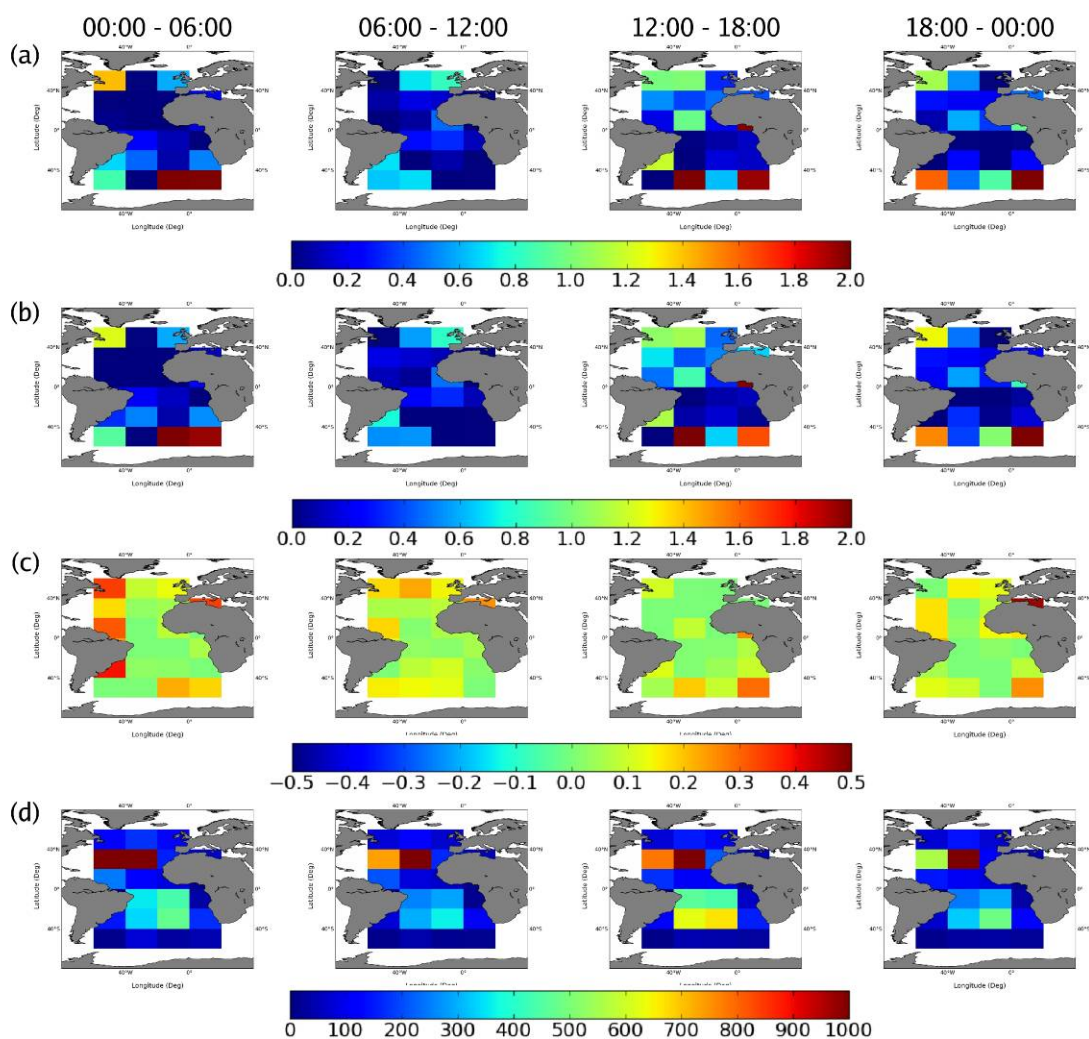


Figure 7: Binned and averaged matchup data for July 2008, bins are 20° by 20° in size. The top two rows show the area averaged SST as measured by (a) the SEVIRI matchups and (b) the drifter matchups; to emphasise the diurnal cycle the minimum SST for the day has been removed from each bin. Row (c) shows the mean difference between the SEVIRI and drifter data. Row (d) shows the number of matchups in each bin. Different columns show the results for different times during the day.

To get a more in-depth analysis of the diurnal signal present in our matchup data, we have performed an hourly analysis on the most densely sampled SEVIRI region (20-40N by 40-20W, see Figure 7). For completeness we also conducted an hourly analysis on the matchup data available for this region from the other satellites. The results of this analysis are shown in Figure 8. In this figure we show hourly values for both the mean SST and the mean difference between the satellite and drifter observations. So that the statistical significance of our results can be assessed, 2 standard errors either side of the mean values are shown (for Gaussian data these are the 90% confidence intervals). In the SEVIRI data a clear diurnal cycle can be seen with a rapid rise in temperature from about 09:00. As witnessed in figure 7, the diurnal cycle is not matched by a diurnal cycle in bias. The bias signal behaves quite differently, with a sudden negative shift in bias at 10:00.

A diurnal signal in the other satellites is much less clear. The large data gaps, due to sun synchronous satellites only ever sampling one part each day and night, make it very difficult to discern a diurnal cycle. However, even taking this into account, only the AVHRR satellite displays a diurnal signal; AATSR and METOP have, respectively, peaks too early in the morning and too late at night. The AVHRR data shows, within errors, a peak at the correct time of the day, with lower temperatures at night. Of note in the AVHRR plots is the peak in bias at the same time as the SST peak; this is a possible indication that for AVHRR the SST diurnal cycle is having an impact on its bias.

Why the AATSR and METOP data do not display a diurnal cycle in Figure 8 needs to be investigated further. However, SSTs (not shown) from the matched drifter data show very similar behaviour, an indication that the odd behaviour of the SST is the result of sampling issues – either temporal or spatial – rather than a problem with the instruments. Nonetheless these problems do highlight the difficulty in extracting diurnal signal and its characteristics from the matchup database we have produced.

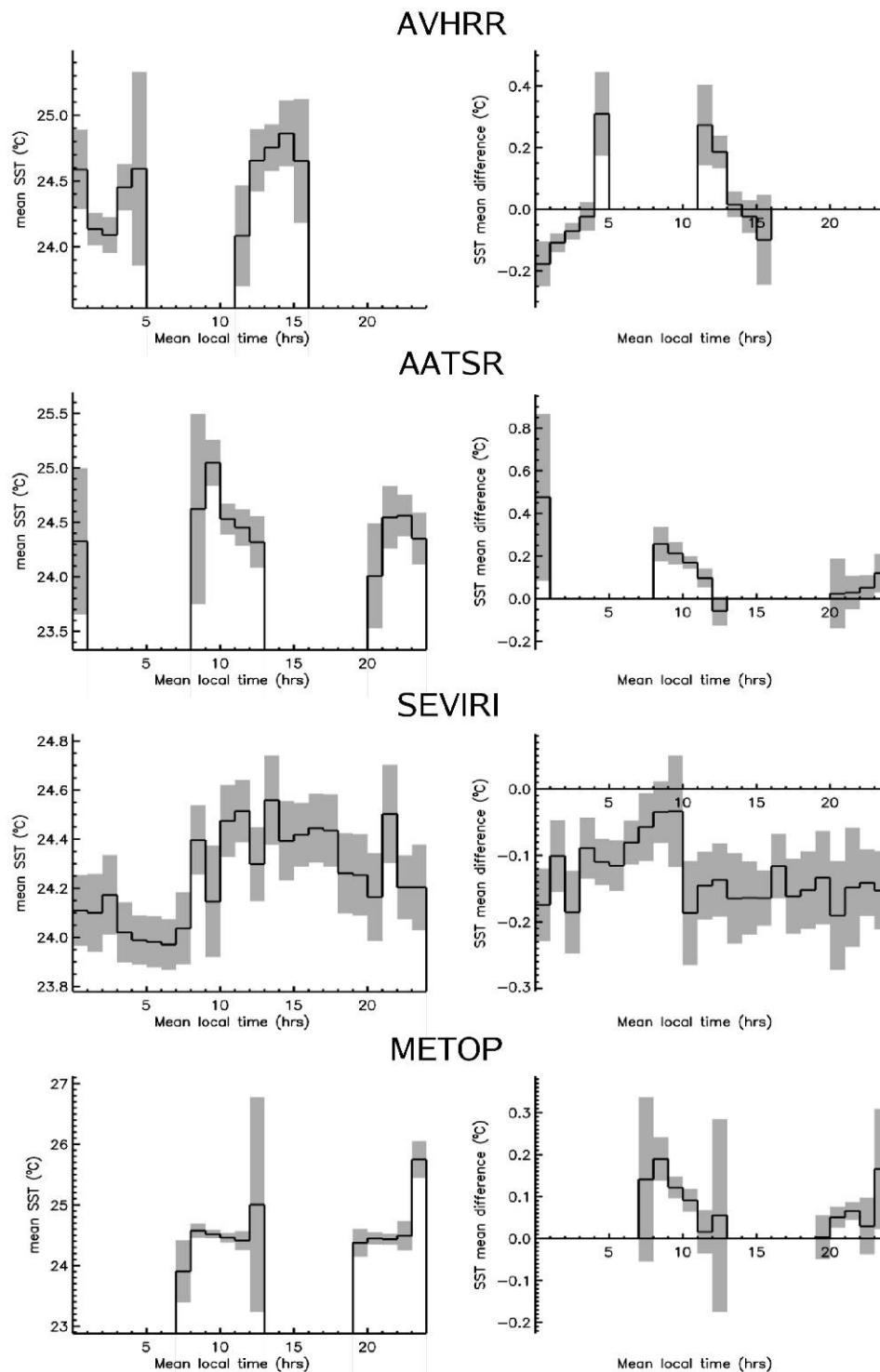


Figure 8: Binned and averaged matchup data from July 2008 for the box 20N-40N, 40W-20W. The left hand plots show the mean satellite SST against the mean local time, while the right hand plots show the equivalent for the mean difference between the drifters and satellites. Each row shows the results for the satellite indicated. All data were binned into 1 hour bins. Grey bars denote 2 standard errors either side of the mean value.

Model Assessment

Model Experimental Setup

The model to be assessed in this study is the Met Office's ORCA025 configuration of NEMO (Nucleus for European Modelling of the Ocean) -FOAM (Forecasting Ocean Assimilating Model). The ORCA025 configuration was developed by Mercator-Océan and consists of a tri-polar NEMO global configuration on a 0.25° (28km) latitude-longitude grid near the equator which reduces to a 6km resolution at high latitudes. The model has 50 depth z-levels with the top box at 1m depth. There is an increased number of levels near the sea surface in order to allow the model to simulate shallow mixed layers and to resolve diurnal variability. The model has temperature, salinity, sea level anomaly (SLA) and sea ice data assimilation performed on the analysis part of each operational run. The model is forced at the surface with meteorological information for heat and moisture fluxes, wind stress and reference temperature using the Met Office Numerical Weather Prediction (NWP) model. Until November 2010, this forcing was 6 hourly but since then the forcing has been increased to 3 hourly. River inputs are also included in the model using climatological data. In addition, the Louvian-le-Neuve sea-ice model (LIM2) is coupled to NEMO-FOAM.

The NEMO-FOAM configuration has been running operationally at the Met Office since December 2008, replacing the previous FOAM system which used the Met Office UM (Unified Model) and had been running since 1997. The model produces global ocean forecasts out to 5 days of various prognostic variables such as temperature, salinity, currents, mixed layer depth and sea ice. See Storkey et al. (2010) for further detailed information about the NEMO-FOAM system.

The model 0 day forecast (known as the analysis) has been assessed in addition to forecast days 1 to 5. The analysis data is not currently provided to defence customers so the analysis results may be ignored for application purposes. It is however important to assess the analysis in order to understand how forecasts can be improved in the future. The analysis is from this point onwards referred to as the 0 day forecast.

For this study a hindcast version of the operational ORCA025 NEMO-FOAM configuration was used. One notable point here is that although the operational version now includes meteorological forcing at a 3 hourly interval, data at this frequency was not available for the hindcast and so 6 hourly fluxes have been used. SST data was output

by the model every hour using a 20 minute time step. The model was run in hindcast mode for July 2008 and February 2009.

Statistics presented in this study are the root-square mean error of the model to observation values (referred to as RMS or RMS error), the mean of the model to observation errors (referred to as bias) and the Pearson correlation coefficient (referred to as R).

Two sets of model assessment have been performed, one against in-situ data and one against satellite data. These are described in the subsequent two sections.

Model and Buoy Comparisons

Observations Used

In order to assess the diurnal cycle present within the model it is necessary to compare the model data to in-situ data. Therefore the SST results from the model hindcast have been compared against a selection of the in-situ buoy SST data collected as described in observations section earlier in this report and their locations are presented in Figure 9.

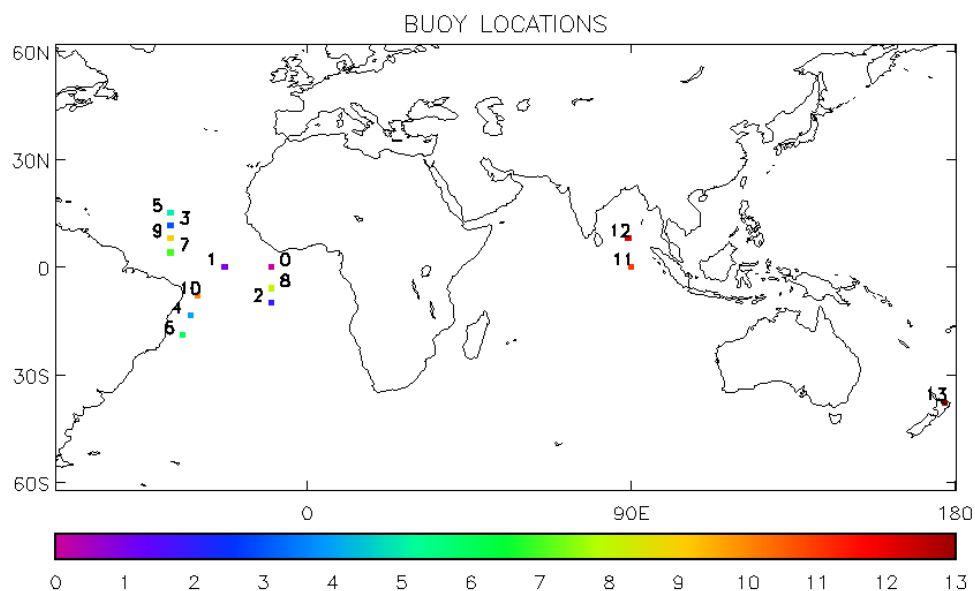


Figure 9: A map showing the locations of the buoys against which the model has been assessed in this report.

Procedure

To compare the diurnal cycle from the model and in-situ data it was decided to investigate the diurnal SST range from both datasets. In order to calculate the diurnal range it is necessary to determine the diurnal maximum and minimum SST values on each day. This is a trivial task by eye, however due to the large size of the datasets it was necessary to construct an algorithm to search the datasets and identify the maximums and minimums automatically. Both the model data at the buoy locations and the buoy data itself were passed through the algorithm. The algorithm functions as follows:

1. Data time is adjusted to local time by offsetting the supplied GMT timings by 1 hour for every 15° of longitude from the Greenwich Meridian.
2. The multi-day time series is split into individual 1 day (24 hour) series which are then searched for minimum and maximum diurnal SST values.
3. The following criteria are applied by the algorithm:
 - the minimum value must occur between 01:00 and 11:00 (local time)
 - the maximum value must occur between 11:00 and 21:00 (local time)
 - the maximum must be greater than the minimum (to remove false detections during days when there is only a cooling SST trend)
 - the maximum/minimum values must have valid data 1 hour before and 1 hour after
 - if multiple minima are detected the latest (in time) is used
 - if multiple maxima are detected the earliest (in time) is used
 - the maximum and minimum as well as the time of day of each are stored.
4. Diurnal ranges are then calculated (maximum-minimum) where valid maximum and minimum values have been identified.

As described in the introduction of this report, the diurnal cycle consists of a minimum in SST around dawn as a result of the night-time cooling after which the SST increases to a maximum in the afternoon due to the solar heating; hence the time restriction on the maximum and minimum values in the algorithm mentioned above. The time window requirement of 1 hour of data either side of the maximum or minimum is necessary to provide some form of data quality assessment. If any given 1 day time series has too few consecutive data points then it is likely the diurnal maximum and minimum will not be captured due to a lack of information and so is discounted from this assessment.

Different time windows were tested prior to use here (not presented) and it was found that a 1 hour window was sufficiently strict to maintain data quality but at the same time not too restricting to result in an excessive amount of 1 day time series' being discarded.

Hourly Time Series

An example time series comparison of the model forecasts compared to buoy data is presented in Figure 10. From this time series it is clear the hourly buoy data is of sufficient quality to capture the diurnal cycle with repeated SST warming and cooling events present throughout the study period. Some days show greater diurnal variability than others depending upon the amount of solar radiation received, the wind speed and the amount of surface water mixing present on individual days. The model displays diurnal variability and shows similar variability to that seen in the observed buoy data at this location; although it does less well at other buoys (not shown). In general there is a bias in the model SST compared to the buoy; this bias being different for each forecast lead time (see the following sub-sections). In order to determine which forecast time does the best overall job of capturing the diurnal variability and to assess the model in detail, further analysis was performed.

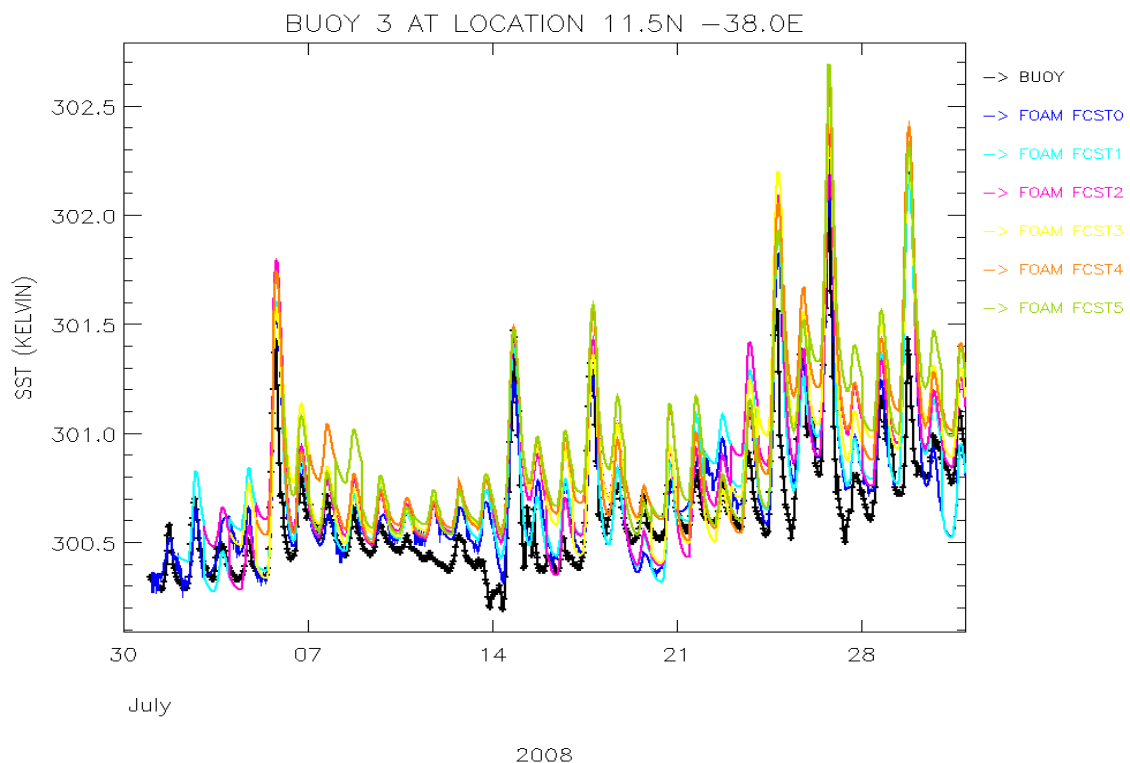


Figure 10: Hourly time series of SST from buoy 3 (black) and the nearest model point (and time) using the model 0 (dark blue), 1 (light blue), 2 (pink), 3 (yellow), 4 (orange) and 5 (green) day forecast. All units in Kelvin.

Diurnal Maxima, Minima and Ranges

The diurnal maximum/minimum algorithm was applied to the buoy and model time series data; the results of this can be seen in Figure 11. The algorithm has captured maxima, minima and therefore ranges for all days of July 2008; with clear variability in the magnitude of the diurnal range. From the time series for buoy 3 shown in Figure 10 there were 6 particularly clear and large diurnal events during the July period, these being on 5th, 14th, 17th, 24th 26th and 29th. These 6 large events have been captured well by the algorithm producing greater diurnal ranges for the buoy data of between 0.75 and 1.4K than on the other days. The model captured these same 6 events for all forecast lead times although it overestimated 4 of the 6.

In general the model (at all forecast times) captures the maximum values well at buoy 3 with high correlations (greater than 0.9) and low biases (around 0.25K). The correlations increase with forecast time although the RMS errors and biases also increase; this is not true of all buoys as stated in Table 2. The minimum values are captured less well at this buoy in terms of variability with correlations less than 0.8, and the correlations now decrease with increasing forecast time. The RMS errors are similar to that of the maxima being around 0.25K. Both minima and maxima are generally overestimated at this site and all the other buoys (see Table 2).

The model diurnal ranges are generally captured well with reasonably high correlations against buoy 3; these being greater than 0.88 for all forecasts. The biases and RMS errors are similar for all forecast times.

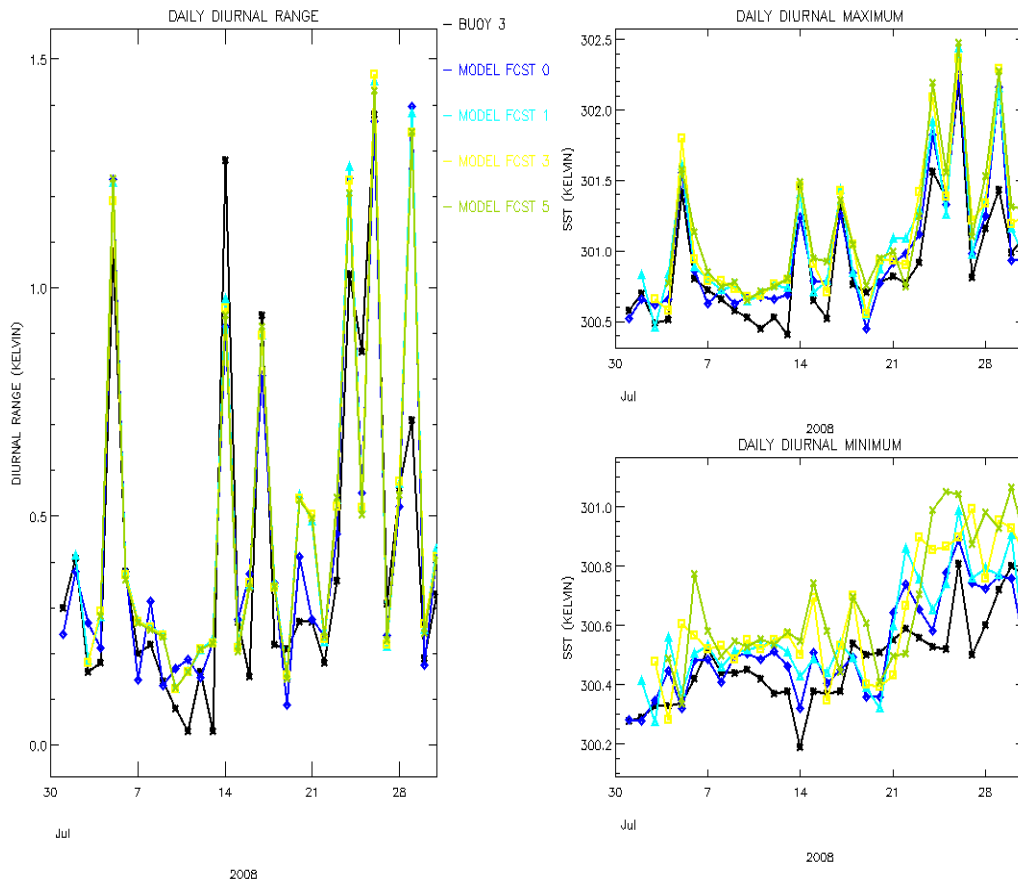


Figure 11: Daily time series of buoy and model (using 0, 1, 3 and 5 day forecast data) diurnal maximum (top right), minimum (bottom right) and range (left) values at the buoy 3 location. All units in Kelvin.

Data from all the deep water buoys (i.e. buoys 0 to 12) were collected together to allow statistics across all buoys to be calculated. Only the data for the deep water buoys were used as the model is a deep water model. Anomaly correlations have been calculated for the diurnal maximum and minimum comparisons in order to only assess the temporal rather than spatial correlation of the model to the buoys. The results from the combined dataset is presented in Table 2.

There is a small warm bias of the order 0.01 to 0.1K in the model minimum and maximum diurnal SST values compared to the buoys; this bias is present at all forecast lead times. Biases and RMS errors for the maxima and minima increase with forecast lead time. Correlations decrease with increasing forecast time from approximately 0.7 for the 0 day forecast to 0.6 for the 1-5 day forecasts.

In contrast the correlations of the diurnal ranges increase by approximately 0.1 between the 0 day and the 1-5 day forecasts. The RMS errors and biases of the ranges are less

for forecasts 1, 3 and 5 than 0. The best forecast time in terms of range appears to be the 1 day forecast, although there isn't a large drop in skill out to the 5 day forecast; with the worst being the 0 day forecast.

| | MIN | | | MAX | | | RANGE | | |
|-------|---------|-------|-------|---------|-------|-------|-------|--------|-------|
| FCST | R(ANOM) | BIAS | RMS | R(ANOM) | BIAS | RMS | R | BIAS | RMS |
| FCST0 | 0.754 | 0.044 | 0.263 | 0.727 | 0.008 | 0.299 | 0.463 | -0.036 | 0.238 |
| FCST1 | 0.706 | 0.086 | 0.294 | 0.698 | 0.058 | 0.330 | 0.548 | -0.026 | 0.208 |
| FCST3 | 0.661 | 0.093 | 0.318 | 0.646 | 0.063 | 0.368 | 0.537 | -0.030 | 0.214 |
| FCST5 | 0.608 | 0.097 | 0.357 | 0.613 | 0.070 | 0.395 | 0.558 | -0.027 | 0.209 |

Table 2: Combined statistics of all deep water buoys (buoys 0 to 12) against model 0, 1, 3 and 5 day forecasts for diurnal minima, maxima and range. Bias and RMS error units are in Kelvin.

Maxima and Minima Timing

In addition to the accuracy of the diurnal maxima and minima, it is also important to assess the phasing of these events. Therefore to assess the timings the algorithm (as described previously) stores the time of day at which the diurnal maximum and minimum occurred. At buoy 3 the buoy data indicates that generally the minimum occurs around 06:30 and the maximum occurs around 15:00 (local time). The model 1, 3 and 5 day forecasts tend to agree reasonably well with these timings; however the 0 day forecast consistently predicts the minimum early and the maximum late. There is much less variability in the timings for the 1-5 day forecasts compared to the 0 day.

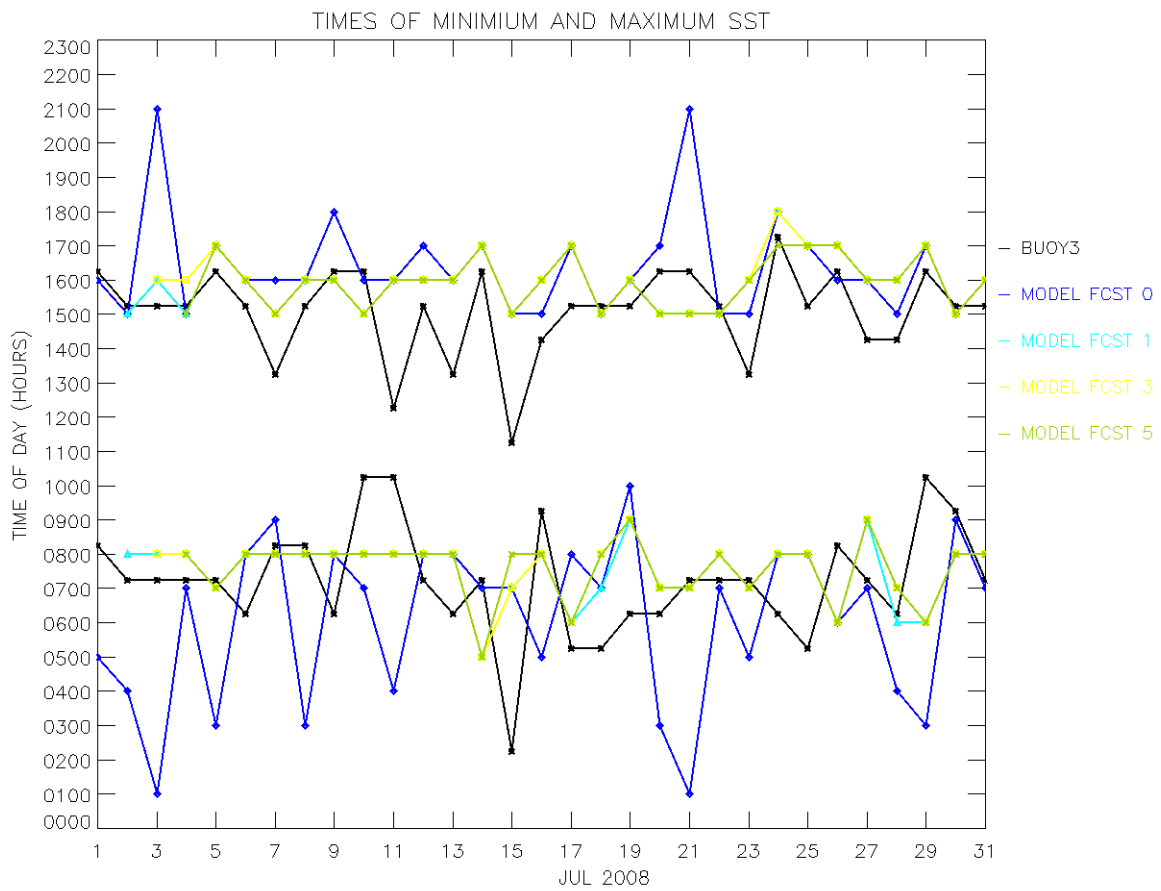


Figure 12: Daily time series of the time of day at which diurnal maximum (top set of lines) and minimum (bottom set of lines) SST was identified by the algorithm at buoy 3 for the buoy and model 0, 1, 3 and 5 day forecast.

From Table 3 it can be seen that the model 0 day forecast predicts an earlier minimum compared to all, except one, of the buoys; the bias of all the buoys taken together being over 1 hour early. In contrast the 1, 3 and 5 day forecasts tend to predict the minimum later than the buoys, the bias across all buoys being around 30 minutes. The 1 day forecast is overall closest to the buoy timings with the 0 day forecast the furthest.

Comparing the timing of the maxima with all the buoys (Table 3) shows that almost all forecast times predict the maxima later than the buoy. Overall all forecasts predict the maximum approximately 1 hour later than the buoy. The 1-5 day forecasts have the lowest biases, all of which being very similar; the 0 day forecast has the largest bias.

| BUOY | MIN | | | | MAX | | | |
|-----------|-------|-------|-------|-------|-------|-------|-------|-------|
| | FCST0 | FCST1 | FCST3 | FCST5 | FCST0 | FCST1 | FCST3 | FCST5 |
| BUOY0 | -1.09 | -1.72 | -1.15 | -1.43 | 1.75 | 1.05 | 0.96 | 1.64 |
| BUOY1 | -0.35 | 0.58 | 0.75 | 0.25 | 0.65 | 0.08 | 0.47 | 0.79 |
| BUOY2 | -3.64 | 0.92 | 0.72 | 0.86 | 1.78 | 2.45 | 2.30 | 2.21 |
| BUOY3 | -1.19 | 0.32 | 0.37 | 0.39 | 1.30 | 0.88 | 0.96 | 0.89 |
| BUOY4 | -2.22 | 0.95 | 0.85 | 0.79 | 0.98 | -0.02 | -0.04 | 0.04 |
| BUOY5 | -1.73 | -0.15 | 0.03 | 0.18 | 0.43 | -0.12 | -0.08 | -0.07 |
| BUOY6 | -1.06 | 2.78 | 2.37 | 2.43 | 1.94 | 0.82 | 0.89 | 0.71 |
| BUOY7 | 0.91 | 1.68 | 1.61 | 1.71 | 0.88 | 0.48 | 0.51 | 0.61 |
| BUOY8 | -0.77 | 1.02 | 1.41 | 1.36 | 0.69 | 0.92 | 0.82 | 0.96 |
| BUOY9 | -0.12 | 0.58 | 0.65 | 0.93 | 1.01 | 0.72 | 0.68 | 0.71 |
| BUOY10 | -2.02 | 0.15 | 0.09 | 0.18 | 1.43 | 0.95 | 0.89 | 1.04 |
| BUOY11 | -1.06 | 0.06 | -0.11 | 0.19 | 2.27 | 1.95 | 1.65 | 1.68 |
| BUOY12 | -1.83 | -0.53 | -0.39 | -0.21 | 2.23 | 1.92 | 1.78 | 1.61 |
| ALL BUOYS | -1.24 | 0.51 | 0.55 | 0.59 | 1.33 | 0.93 | 0.91 | 0.99 |

Table 3: Bias statistics (in hours) of the timing of the minima and maxima of the model compared to each buoy, and all deep water buoys (0-12).

New Zealand Buoy Assessment

The New Zealand buoy is located in water of approximately 65m depth and so in global ocean terms this is a shallow water site. As a consequence it was felt prudent to investigate this buoy location separately. The NEMO-FOAM ORCA025 configuration is a deep water model and so it is to be expected that it would perform less well at such a shallow site, however the global domain does include such shallow regions and so an assessment is still necessary. The data available for this buoy was for a 2 week period at the end of February/beginning of March 2009; however, model data with forecasts was only available for February 2009 and so the assessment presented here is for the last week of February 2009 only.

As can be seen from Figures 13 to 15, even though this is a shallow water region the model performs well at capturing the period of the SST and the diurnal cycle; the timings of the minimums being particularly well matched. The clear shortfall in the model at this location is that the model underestimates the variability of the SST in terms of amplitude and so the model significantly underestimates the diurnal maxima, minima and ranges. A contributing factor to this underestimation by the model maybe due to the fact that the buoy is measuring at a 15-minute frequency compared to the model outputting hourly data. This difference in frequency means that the buoy is more responsive to the surface heating than the model and so will see a greater range of SST values.

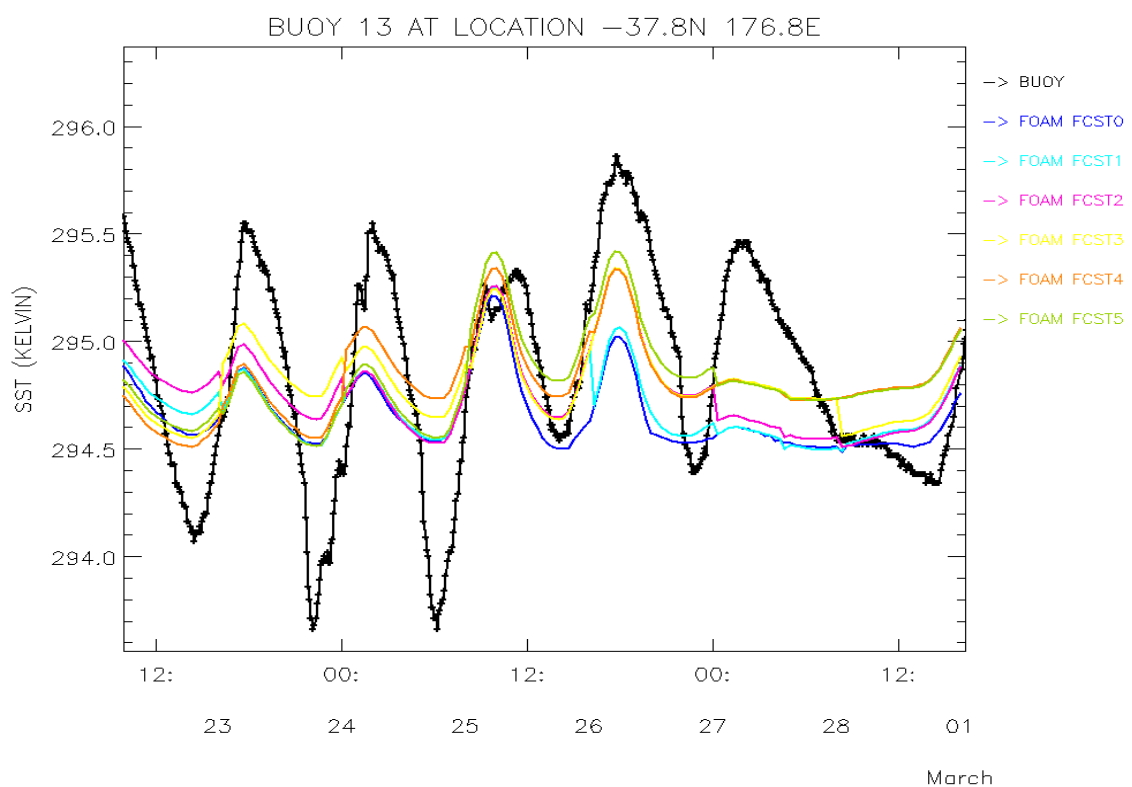


Figure 13: Time series of SST (in Kelvin) at the New Zealand buoy (15 minute) and the model forecasts (hourly).

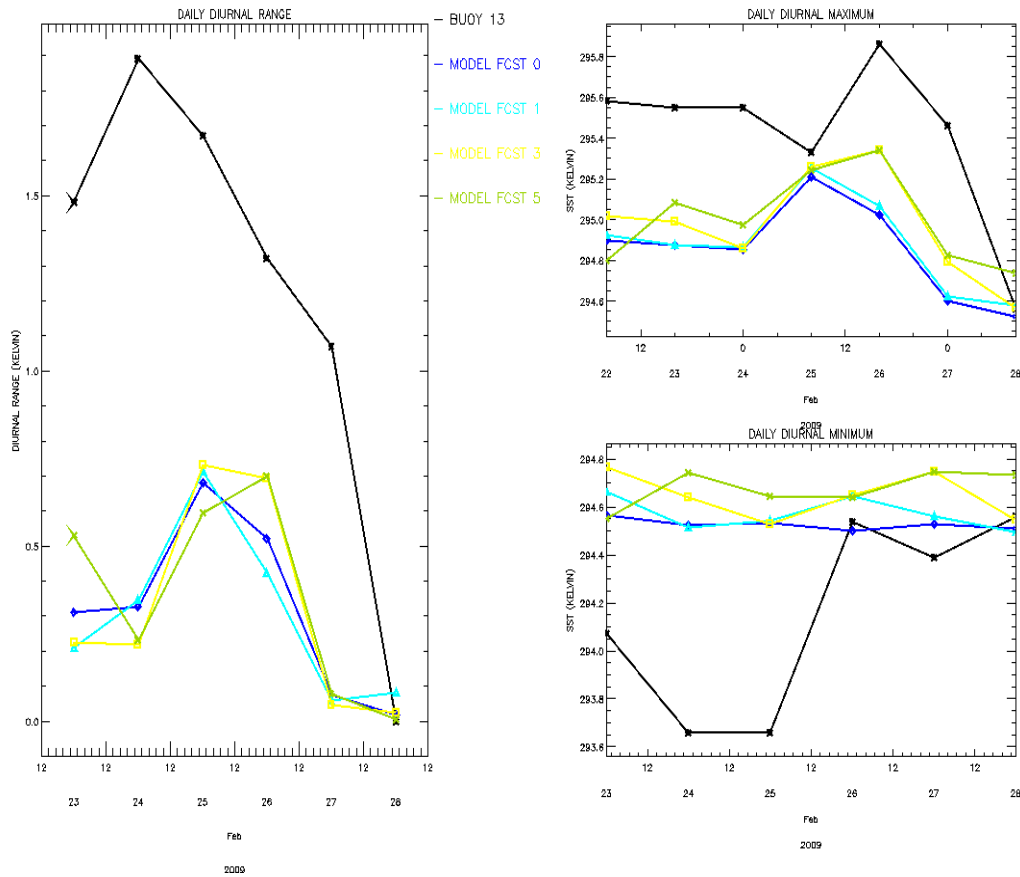


Figure 14: Daily time series comparisons of buoy and model diurnal maxima, minima and ranges (in Kelvin).

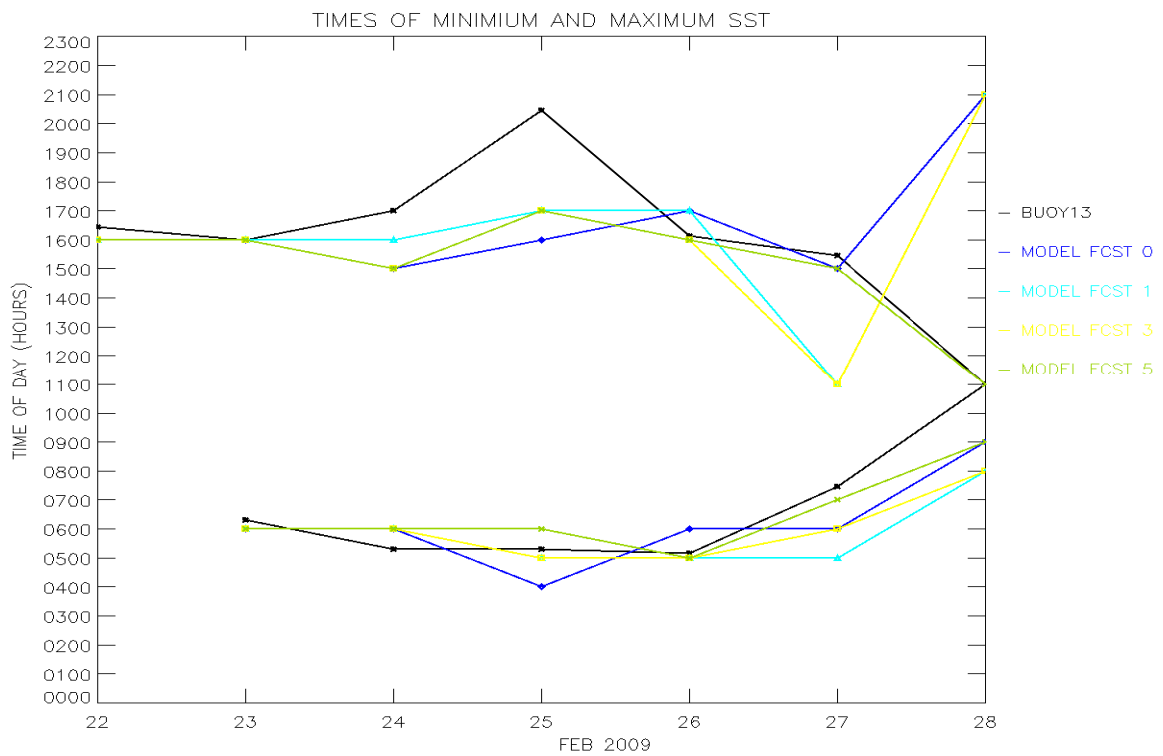


Figure 15: Daily time series comparison of the timing of the diurnal maxima (top set of lines) and minima (bottom set of lines) of the buoy and model.

Model and Satellite Comparisons

Procedure

To allow assessment of the model diurnal cycle over a much greater area than the point measurements of in-situ buoys, comparison against the SEVIRI satellite data was performed. Once the satellite data had been gridded onto a regular 0.25° latitude/longitude grid it was passed through the diurnal maximum/minimum algorithm described in the previous section. Due to potential coverage issues with the satellite data it was decided to extract the model values at the satellite maximum and minimum times to reduce the potential of punishing the model for finding the 'true' diurnal minimum/maximum when the satellite coverage only allowed a local minimum/maximum to be found. Diurnal ranges were then calculated for every grid point of the satellite and model data and for each model forecast lead time.

The information obtained from this procedure was used to produce maps of diurnal maximum, minimum and range values with maps of RMS error, bias, correlation coefficient and number plots of data that were available at each grid point (N).

The correlation plots in Figures 16 to 18 have more missing data than the other statistics plots. This is for 2 reasons: (a) the method by which correlations are calculated; if one of the datasets to be correlated contains only repeated values, that dataset has a variance of 0 and so the correlation coefficient is undefined and (b) a criteria of requiring 5 or more values to be available for the calculation in order to increase the degrees of freedom and so increase the significance of the results.

Statistics Maps

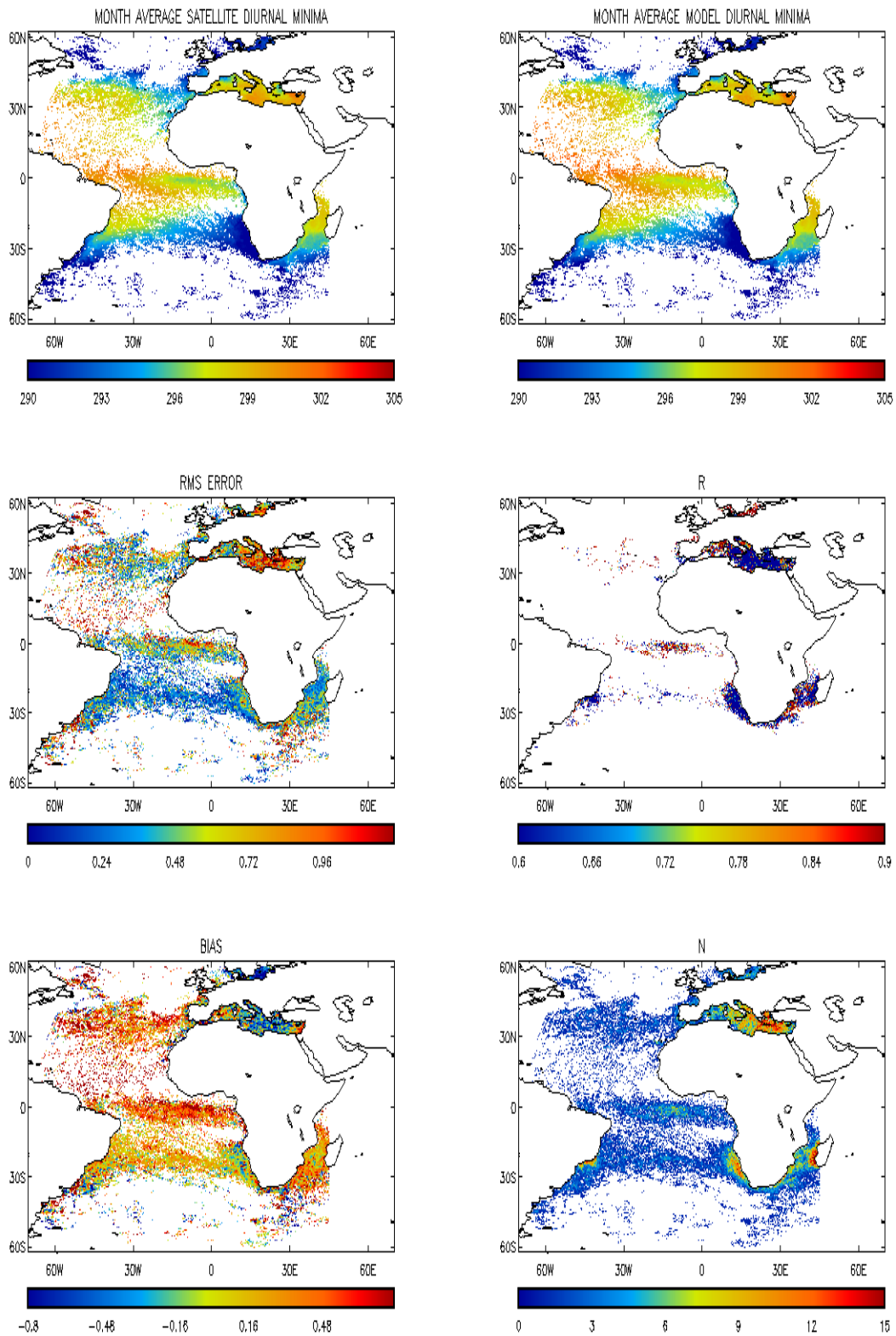


Figure 16: Comparison of satellite and model diurnal minima (1 day forecast) using monthly average minima SST values from the satellite (top left) and model (top right) in Kelvin, RMS error (middle left) in Kelvin, correlation coefficient (middle right), bias (bottom left) in Kelvin and number of days with 'valid' minima (bottom right) values.

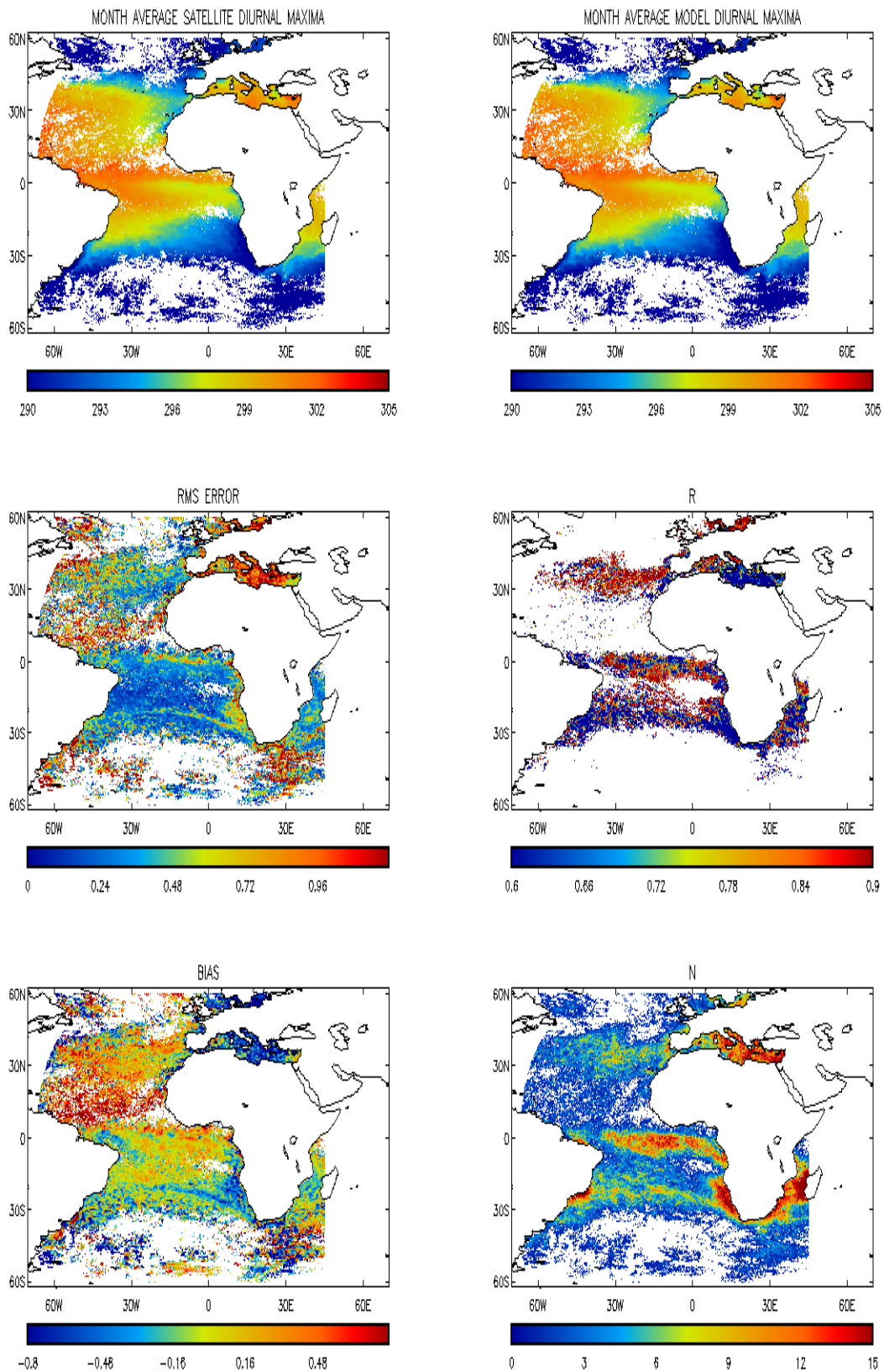


Figure 17: Comparison of satellite and model diurnal maxima (1 day forecast) using monthly average maxima SST values from the satellite (top left) and model (top right) in Kelvin, RMS error (middle left) in Kelvin, correlation coefficient (middle right), bias (bottom left) in Kelvin and number of days with 'valid' maxima (bottom right) values.

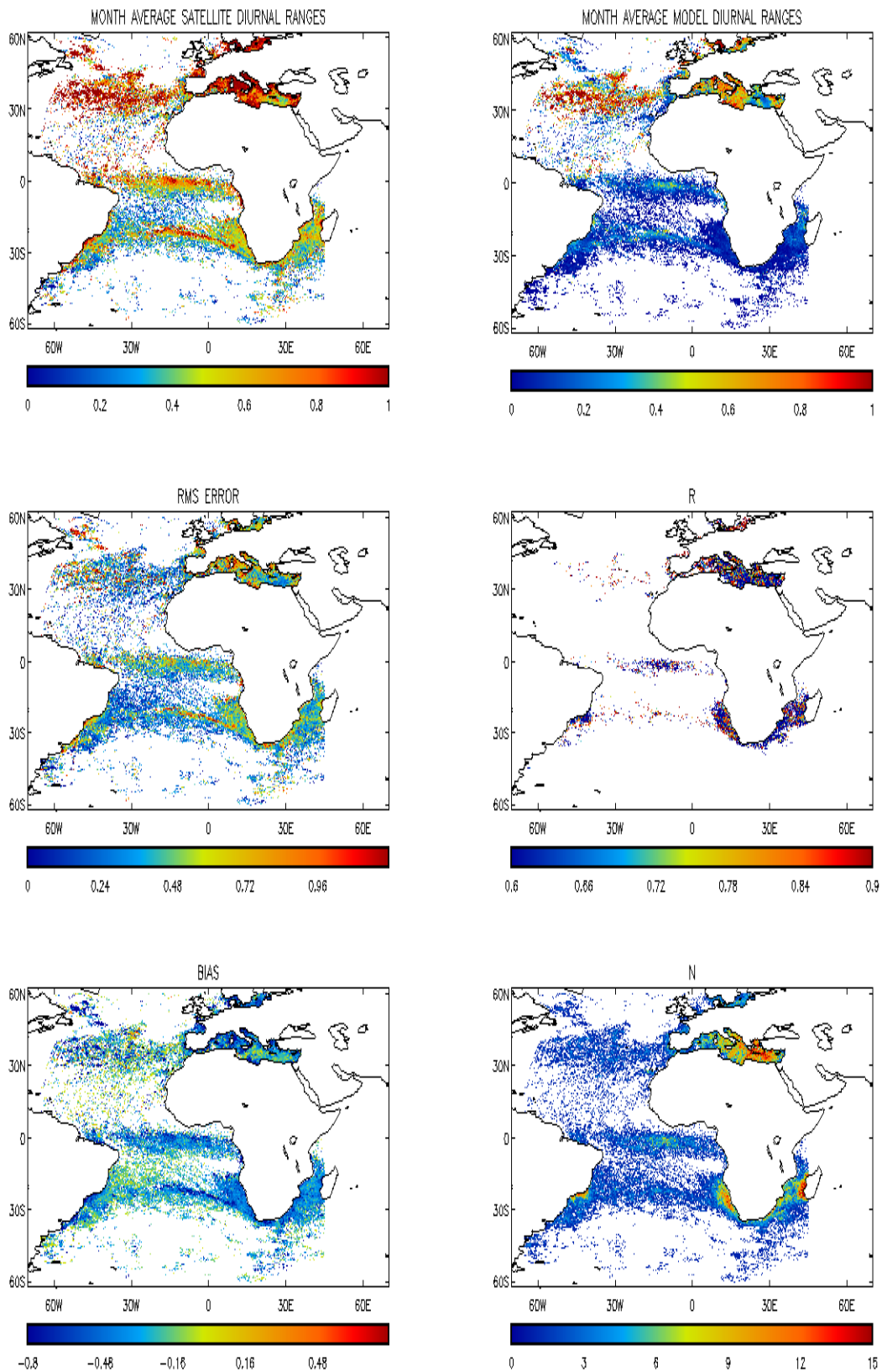


Figure 18: Comparison of satellite and model diurnal range (1 day forecast) using monthly average diurnal range values from the satellite (top left) and model (top right) in Kelvin, RMS error (middle left) in Kelvin, correlation coefficient (middle right), bias (bottom left) in Kelvin and number of days with 'valid' range (bottom right) values.

The statistics maps in Figures 16 to 18 show that there is generally better coverage by the satellite in the afternoon period for diurnal maximum detection than there is in the morning period for diurnal minimum detection; this point is highlighted by comparing the maps of N. This difference in coverage is presumably due to differing cloud conditions between these two times of day.

The month-average values for satellite and model look reasonably similar for the maxima and minima diurnal SST, the statistics however demonstrate that there are differences. There is a warm bias (of the order of 0.2-0.5K) in the minima across the domain, except in the eastern Mediterranean where there is a cold bias of approximately -0.4K. The RMS errors are greatest in the Mediterranean, at higher latitudes and generally nearer the coasts with values between 0.5 and 1K.

Larger areas of the domain (including the Mediterranean) have a cold bias or very little bias in terms of the maxima, these values being between -0.3 and 0; although parts of the North Atlantic still have a warm bias (between 0.2 and 0.6K). The RMS errors of the maxima follow much the same pattern as for the minima.

Although the Mediterranean has cold biases in both the maxima and minima, the resultant diurnal ranges are reasonably close to the satellite predictions with a very slight (of order 0.15K) under-prediction. Both the model and satellite predict bands of larger diurnal range around the 30N, 0N and 30S lines of latitude; these being the regions close to the areas known as the horse latitudes (at approximately 30-35N and 30-35S) and the Equator (0N). The larger diurnal ranges seen in the horse latitudes may be as a result of the low wind speeds due to the sub-tropical high which is characteristic of these latitudes. When the wind speed is low there is a greater degree of sea surface warming and reduced vertical mixing leading to increased diurnal ranges. This relationship between wind speed, mixing and SST has been observed in the western equatorial Pacific warm pool by Soloviev and Lukas (1997) and later by Murray et al. (2000) as well as in the Mediterranean and European shelf seas by Merchant et al. (2008). The model does better at capturing the magnitude of the diurnal ranges near 30N, this possibly due to the time of year as the surface heat flux is greater in the northern hemisphere in July. Almost without exception across the domain the model underestimates the diurnal range. Generally the correlations of the month-average ranges are low although the correlations of the minima and maxima tend to be higher.

Domain-Average Statistics

The information provided by the statistical maps was condensed into statistics for the domain as a whole which are presented in Tables 4 and 5. These domain-average statistics clearly highlight the increased coverage of the maxima compared to the minima; there being approximately a factor of 3 more points at which maxima have been detected than minima throughout the month. Anomaly correlations for the maximums and minimums decrease with increasing forecast time. RMS errors and biases also increase with forecast time in terms of the minimums; however, they both decrease with forecast time for the maximums. The resultant diurnal ranges therefore have similar RMS errors and biases across the forecast times with the model overall underestimating the range by around 0.4K.

The same story is seen in the statistics for satellite and model data for February 2009 although the correlations tend to be lower. The warm bias in the minimums and the cold bias in the maximums tend to be warmer and colder respectively in the February data which results in a more significant underestimation of the ranges.

The model 1 day forecast is arguably the best model forecast time at predicting diurnal range; the 5 day forecast has a slightly better overall correlation, however the RMS errors and bias are worse. The 0 day forecast is consistently worse at predicting the diurnal range as it has the lowest correlations and greatest RMS errors and bias.

| MONTH | FCST | MIN | | | | MAX | | | |
|--------|-------|---------|-------|-------|---------|---------|--------|-------|---------|
| | | R(ANOM) | BIAS | RMS | N | R(ANOM) | BIAS | RMS | N |
| Jul-08 | FCST0 | 0.555 | 0.087 | 0.722 | 123,659 | 0.620 | -0.208 | 0.731 | 393,693 |
| | FCST1 | 0.499 | 0.114 | 0.747 | 121,468 | 0.606 | -0.136 | 0.713 | 382,744 |
| | FCST5 | 0.424 | 0.229 | 0.738 | 106,769 | 0.538 | -0.063 | 0.700 | 334,179 |
| Feb-09 | FCST0 | 0.488 | 0.147 | 0.633 | 72,798 | 0.520 | -0.264 | 0.703 | 320,537 |
| | FCST1 | 0.444 | 0.159 | 0.654 | 70,664 | 0.537 | -0.209 | 0.694 | 309,755 |
| | FCST5 | 0.358 | 0.184 | 0.696 | 61,567 | 0.495 | -0.181 | 0.715 | 266,152 |

Table 4: Domain-average diurnal minimum and maximum statistics of satellite against model 0, 1 and 5 day forecasts for July 2008 and February 2009.

| MONTH | FCST | RANGE | | | |
|--------|-------|-------|--------|-------|---------|
| | | R | BIAS | RMS | N |
| Jul-08 | FCST0 | 0.468 | -0.471 | 0.677 | 123,659 |
| | FCST1 | 0.673 | -0.397 | 0.564 | 121,468 |
| | FCST5 | 0.678 | -0.412 | 0.573 | 106,336 |
| Feb-09 | FCST0 | 0.553 | -0.477 | 0.655 | 72,798 |
| | FCST1 | 0.646 | -0.439 | 0.603 | 70,664 |
| | FCST5 | 0.654 | -0.445 | 0.606 | 61,288 |

Table 5: Domain-average diurnal range statistics of satellite against model 0, 1 and 5 day forecasts for July 2008 and February 2009.

Conclusions.

The aim of this study was to investigate current ability to determine the diurnal cycle of SST using remote observations such as buoys and satellites, and using a numerical model, in this case the FOAM global model.

The buoy data used in this study is generally effective at capturing the diurnal cycle as they sample at a rate of hourly or greater. One important point about the buoys is that their measurement of SST is typically at a depth of 1m and so the measurements are not the 'true' skin temperature. Another drawback to using buoys is that they do not have the good spatial coverage of satellites and models.

Assessment of the ability of satellites to observe SST and the diurnal cycle highlighted the important issue of coverage that satellites provide. In order to potentially capture the diurnal cycle it is necessary to use geostationary satellites such as SEVIRI, but even with these, the presence of cloud means a sufficient sampling rate still may not be possible. It was found that a minimum of 1 satellite sample from each of the 4 equally spaced 6 hour periods (defined in the sampling requirements part of this document) per day are required to capture the diurnal SST cycle. However even with a geostationary satellite capturing 4 samples per day is not necessarily possible.

When sufficient satellite coverage is available the diurnal signal observed is comparable to that measured by in-situ buoys. The advantages of satellite data over buoy data are that satellites often give a true skin SST measurement and their geographical coverage is much greater. The overall error in the satellite data compared to drifters is of the order of 0.1K or less with standard deviations in the between 0.4 to 0.7K.

The assessment of the FOAM global model has produced some promising results but has also highlighted the system's limitations and areas for future development. Comparison against in-situ buoys showed promising results with all forecast lead times able to predict to some degree of accuracy a diurnal cycle. The diurnal range was generally underestimated by all forecast times which is thought to be partly due to the effects of using the 6 hourly forcing rather than 3 hourly. Experiments using 3 hourly forcing (not presented here) rather than 6 hourly suggest that the diurnal range is increased by the higher forcing frequency.

The model's ability to predict the timing of the diurnal cycle was also promising with the model being half an hour late on average for the minimum and 1 hour late for the maximum for the 1-5 day forecasts when compared to the buoys.

The timings and diurnal range predictions were worse for the 0 day forecast which is believed to be to do with the way in which data assimilation of temperature is performed on this model day. The assimilation increments are applied throughout the model day and so this has a constraining effect. It is worth stating again that the 0 day forecasts are not provided to defence customers and the results in themselves are less important than for the 1-5 day forecasts. However, further work on the initialisation of SSTs could possibly also result in improved forecasts.

Comparison of the model to the SEVIRI satellite data showed that the underestimation in diurnal SST range is not just limited to the buoy locations but is generally true. The model does, however, capture to some degree the regions of larger diurnal range associated with the horse latitudes and the Equator. Overall the 1 day forecast emerges as the best forecast lead time, although there isn't a big difference in skill between the 1 to 5 day forecasts.

It is worth stating that no skin correction has been applied to the model data in order to estimate the sea surface skin temperature (the parameter that the SEVIRI satellite is

measuring); the top model box has been used which is at 1m depth. The skin temperature is more variable than the sub-surface temperature as it is more responsive to the high frequency variations in surface heating. The sub-surface temperatures respond on a slower scale once mixing has transported the heat to depth. This means that the satellite skin temperature data tends to produce greater diurnal ranges than the model at 1m depth.

Future Work and Recommendations

As a result of this report it is suggested that a study be carried out to develop a system that combines the satellite SST data with a diurnal SST model that would be capable of operationally providing global maps of diurnal cycle each day. The combination of a 1D diurnal model (examples of which are referred to in the introduction of this report) with the data would enable more robust estimates of diurnal variability to be made in the presence of sparse observations. This diurnal analysis would be done in the context of the existing OSTIA system, and would provide a diurnal estimate on top of, and consistent with, the existing foundation SST analysis.

In addition to this development, further work is required to incorporate a 1D skin correction model into the NEMO-FOAM system. This would allow NEMO-FOAM to produce better forecasts of diurnal cycles, thereby improving the information available to customers, and the information used to force atmospheric models. A further assessment of the current model using 3 hourly forcing rather than 6 hour forcing used here would also be useful to provide greater insight into the current skill of the model at predicting diurnal SST.

The recommendation from this study is that diurnal cycle information produced by the 1-5 day forecasts from NEMO-FOAM is of sufficient quality for use by the Navy (with the caveats outlined in this document).

References

Clayson, A. A. and D., Weitlich., 2005. Diurnal warming in the tropical pacific and its interannual variability. *Geophysical Research Letters.*, 32, L21604.

Donlon, C. J., Martin, M., Stark, J. D., Roberts-Jones, J., Fiedler E., In Press. The Operational Sea Surface Temperature and Sea Ice Analysis (OSTIA) system. *Remote Sensing of the Environment.*

Fairall, C. W., Bradley, E. F., Godfrey, J. S., Wick, G. A., Edson, J. B., and S., Young G., 1996. Cool-skin and warm-layer effects on sea surface temperature. *J. Geophys. Res.*, 101, 1295–1307.

Gentemann, C. L., Donlon, C. J., Stuart-Menteth, A., and Wentz, F. J., 2003. Diurnal signals in satellite sea surface temperature measurements. *Geophysical Research Letters.*, 30, 40/1 - 40/4.

Ingleby, B. and Huddleston, M., 2007. Quality control of ocean temperature and salinity profiles—historical and real-time data. *Journal of Marine Systems*, 65, 158–175.

Le Borgne, P., Legendre, G., Marsouin, A., Piéré, S., and A., Philippe., 2011. Operational SST retrieval from MSG/SEVIRI and GOSE-E new chain validation report. *Ocean & Sea Ice SAF Technical report.*

Locarnini, R. A., Mishonov, A.V., Antonov, J. I., Boyer, T. P., and Garcia, H. E., 2006. Volume 1: Temperature. In *World Ocean Atlas 2005 (Levitus, S. ed.)*. U.S government printing office. available at <http://www.nodc.noaa.gov/OC5/WOA05/>.

Lorenc, A. C. and Hammon, O., 1988. Objective quality control of observations using Bayesian methods. theory, and a practical implementation. *Q. J. Roy Met Soc*, 114, 515–543.

Merchant, C. J., J., Filipiak M., Le Borgne, P., Roquet, H., Autret, E., J.-F., Piollé, and, Lavender S., 2008. Diurnal warm-layer events in the western Mediterranean and European shelf seas. *Geophysical Research Letters.*, 35, L04601.

Murray, M.J., Allen, M.R., Merchant, C.J., Harris, A.R. and Donlon, C.J., 2000. Direct observations of Skin-Bulk SST variability. *Geophysical Research Letters*, 27 (8), 1171-1174.

OSI-SAF, 2006. Atlantic sea surface temperature product manual - version 1.6. *EUMETSAT OSISAF Technical report*. Available from <http://www.osi-saf.org/>

OSI-SAF, 2010. Low earth obiter sea surface temperature product user manual - version 2.2. *EUMETSAT OSISAF Technical report*. Available from <http://www.osi-saf.org/>

Percival, D. B. and Walden, A. T., 1993. Spectral Analysis for physical applications—multitaper and conventional univariate techniques. *Cambridge University Press*.

Price, J. F. and Weller, R. A., 1986. Diurnal cycling: observations and models of the upper ocean response to diurnal heating, cooling and wind mixing. *J. Geophys. Res.*, 91, 8411–8427.

Soloviev, A. and Lukas, R., 1997. Observations of large diurnal warming events in the near-surface layer of the western equatorial Pacific warm pool. *Deep Sea Research Part 1: Oceanographic Research Papers*, 44 (6), 1055-1076.

Storkey, D., Blockley, E.W., Furner, R., Guiavarc'h, C., Lea, D., Martin, M.J., Barciela, R.M., Hines, A., Hyder, P. and Siddorn, J.R., 2010. Forecasting the ocean state using NEMO: The new FOAM system. *Journal of Operational Oceanography*, 3 (1), 3-15.

Stuart-Menteth, A. C., Robinson, I. S., and G., Challenor P., 2003. A global study of diurnal warming using satellite-derived sea surface temperature. *J. Geophys. Res.*, 108, 24–1 – 24–12.

Stuart-Menteth, A. C., Robinson, I. S., Wellar R. A., Donlan, C. J., 2005. Sensitivity of the diurnal warm layer to meteorological fluctuations part 1: observations. *Journal of Atmospheric & Ocean Science*, 10, 193 - 208.

Webster, P. J., Clayson, C. A., and Curry, J. A., 1996. Clouds, radiation and the diurnal cycle of sea surface temperature in the tropical western pacific. *Journal of climate*, 9, 1712–1728.

Met Office
FitzRoy Road, Exeter
Devon EX1 3PB
United Kingdom

Tel (UK): 0870 900 0100 (Int) : +44 1392 885680
Fax (UK): 0870 900 5050 (Int) :+44 1392 885681
enquiries@metoffice.gov.uk
www.metoffice.gov.uk